SuperWASP observations of the 2007 outburst of Comet 17P/Holmes

Published in:
Monthly Notices of the Royal Astronomical Society

Document Version:
Peer reviewed version

Queen's University Belfast - Research Portal:
Link to publication record in Queen's University Belfast Research Portal

SuperWASP observations of the 2007 outburst of Comet 17P/Holmes

Henry H. Hsieh,[1]⋆ Alan Fitzsimmons,[1] Yogesh Joshi,[1,2] Damian Christian[1,3] and Don L. Pollacco[1]

[1]*Astrophysics Research Centre, Queen's University, Belfast BT7 1NN*
[2]*Aryabhatta Research Institute of Observational Sciences, Manora Peak, Nainital 263129, India*
[3]*Physics & Astronomy Department, California State University Northridge, Northridge, CA 91330-8268, USA*

ABSTRACT

We present wide-field imaging of the 2007 outburst of Comet 17P/Holmes obtained serendipitously by SuperWASP-North on 17 nights over a 42-night period beginning on the night (2007 October 22–23) immediately prior to the outburst. Photometry of 17P's unresolved coma in SuperWASP data taken on the first night of the outburst is consistent with exponential brightening, suggesting that the rapid increase in the scattering cross-section of the coma could be largely due to the progressive fragmentation of ejected material produced on a very short time-scale at the time of the initial outburst, with fragmentation time-scales decreasing from $t_{\text{frag}} \sim 2 \times 10^3$ to $\sim 1 \times 10^3$ s over our observing period. Analysis of the expansion of 17P's coma reveals a velocity gradient suggesting that the outer coma was dominated by material ejected in an instantaneous, explosive manner. We find an expansion velocity at the edge of the dust coma of $v_{\text{exp}} = 0.55 \pm 0.02$ km s^{-1} and a likely outburst date of $t_0 = 2007$ October 23.3 ± 0.3, consistent with our finding that the comet remained below SuperWASP's detection limit of $m_V \sim 15$ mag until at least 2007 October 23.3. Modelling of 17P's gas coma indicates that its outer edge, which was observed to extend past the outer dust coma, is best explained with a single pulse of gas production, consistent with our conclusions concerning the production of the outer dust coma.

Key words: comets: general – comets: individual: 17P/Holmes.

1 INTRODUCTION

Discovered on 1892 November 9 by Edwin Holmes, Comet 17P/Holmes (hereafter, 17P) is a dynamically ordinary Jupiter-family comet, with a semimajor axis of $a = 3.617$ au, an eccentricity of $e = 0.432$, an inclination of $i = 19°.11$, an orbital period of $P_{\text{orb}} = 6.8$ yr and a Tisserand parameter (with respect to Jupiter) of $T_J = 2.859$. On 2007 October 24.1, it was discovered by J. A. Henríquez Santana to be undergoing a substantial outburst. Starting from an initially observed magnitude of $m_V \sim 8.4$ (compared to a pre-outburst brightness of $m_V \sim 17$ measured on 2007 October 23.1; Casali et al. 2007), it brightened by approximately 0.5 mag h^{-1} over the course of 6 h (Buzzi et al. 2007). The comet reached $m_V \sim 2.0$ by 2007 October 25.1 (Sposetti et al. 2007; El-Houssieny, Nemiroff & Pickering 2010), representing a million-fold increase in brightness over only 2 d. This outburst of 17P mirrored a similar outburst that led to the comet's initial discov-ery in 1892, and continued to be monitored by both amateur and professional astronomers as it progressed.

Spectroscopic analyses indicated that the coma was largely dominated by dust grains (Schleicher 2007), but evidence of cometary volatiles and sublimation byproducts, including OH, H_2O, NH, CN, HCN, HNC, C_2, C_3, C_2H_2, C_2H_6, CS, CH_3CN and CH_3OH, were also detected during the outburst (Drahus et al. 2007; Fitzsimmons, Snodgrass & Southworth 2007; Kobayashi, Kawakita & Nishikoji 2007; Schleicher 2007; Wagner et al. 2007; Bockelée-Morvan et al. 2008; Dello Russo et al. 2008; Yang, Jewitt & Bus 2009). Negative polarization was found for the dust coma by Joshi, Ganesh & Baliyan (2010), consistent with measurements made for other comets. A delay in the appearance of CN, C_2 and [O I] emission lines between 2007 October 24.58 and October 25.46 led Kobayashi et al. (2007) to speculate that their observations could be at least partially explained by the delayed sublimation of icy grains ejected at the time of the outburst. This hypothesis is supported by Dello Russo et al. (2008) who found evidence of a distributed source of sublimation products, consistent with the ejection and subsequent delayed sublimation of icy grains in the coma. The total mass loss due to this outburst has been estimated to be $\sim 10^{10} - 10^{12}$ kg or up

⋆E-mail: h.hsieh@qub.ac.uk

to a few per cent of the comet's total mass (Montalto et al. 2008; Sekanina 2008a; Ishiguro et al. 2010).

2 OBSERVATIONS AND REDUCTION

The Wide Angle Search for Planets (WASP) operates two facilities: Super-WASP-N (hereafter, SuperWASP), located in the northern hemisphere on La Palma, and WASP-S, located in the southern hemisphere at the South African Astronomical Observatory. These two facilities, comprising eight cameras each, provide fully robotic, high time-resolution, and ultra-wide angle imaging of selected star fields for the primary purpose of detecting transiting extrasolar planets. Each camera employs 200 mm f/1.8 Canon lenses with apertures of 11.1 cm and a broad-band filter defining a custom passband from 400 to 700 nm. The detectors are 2048 × 2048 thinned e2v CCDs with an image scale of 13.7 arcsec pixel^{-1} for a total field of view of 7°.8 × 7°.8 per camera. Images are processed by an automated reduction pipeline that performs bias and thermal dark frame subtraction and flat-field reduction (Pollacco et al. 2006).

SuperWASP serendipitously observed 17P in one camera on numerous nights during the comet's 2007 outburst, starting on the night of 2007 October 23–24 and continuing through 2007 December 2–3, providing us with a well-sampled, long-baseline data set for analysing the comet's evolving brightness and morphology. We list details of these observations in Table 1 and show typical images of the comet obtained on each night of observations in Fig. 1. Data from the night prior to the outburst (2007 October 22–23) is also available. Inspection of these data shows no evidence of the comet at its expected position, indicating that the comet remained below SuperWASP's detection threshold ($m_V \sim 15$ mag) until at least 2007 October 23.3.

On the first night of 17P's outburst, a total of 84 images, comprising 30 s of exposure time each, were obtained from 2007 October 23.9851 (UT 23:38) to October 24.2681 (UT 06:26). Images were obtained in consecutive pairs approximately every 10–12 min. The steadily brightening comet was visible from the start of the observations but became saturated on the CCD from approximately October 24.1496 onwards, leaving 44 images from which reliable photometry could be obtained. The full width at half-maximum (FWHM) measured for field star surface brightness profiles during the period of observations was approximately 23.3 arcsec. Aperture photometry was performed on the comet using apertures with radii of 70.0 arcsec. The background sky flux was measured at several nearby locations on the sky where field star contamination was minimal. Five nearby field stars (within 30 arcmin of the comet) were also measured using the same apertures and used to make differential photometric corrections to our measured comet fluxes to ensure a consistent photometric baseline throughout the observation period.

Because SuperWASP employs a non-standard wide filter optimized for its primary function as a transit detector (Pollacco et al. 2006), precise absolute photometry of 17P in a standard passband is difficult to obtain from this data set. We estimate apparent magnitudes by assuming the spectrum of 17P to be approximately solar and performing differential photometry using nearby FGK-type field stars whose magnitudes and spectral types are known (Table 2). We assign a combined systematic and measurement uncertainty of ∼0.2 mag to these measurements. These magnitudes are computed for comparison to other published results only. All analysis

Table 1. Observation log.

UT date range	Moon[a]	N[b]	R[c]	Δ[d]	α[e]	ν[f]	$pa_{-\odot}$[g]	pa_{-v}[h]	pa_{tail}[i]
2007 Oct 23.0039–Oct 23.2659	N+12	72	2.43	1.64	17.3	61.1	224.8	266.0	–
2007 Oct 23.9851–Oct 24.2681	N+13	84	2.44	1.64	17.0	61.3	223.6	265.8	–
2007 Oct 24.9785–Oct 25.2647	N+14	59	2.44	1.63	16.8	61.6	222.3	265.7	–
2007 Oct 25.9769–Oct 26.1961	N+15	31	2.44	1.63	16.5	61.9	221.0	265.5	–
2007 Oct 31.9649–Nov 01.2547	N–9	78	2.47	1.62	15.0	63.6	212.2	264.3	–
2007 Nov 01.9575–Nov 02.2510	N–8	76	2.47	1.62	14.7	63.9	210.5	264.0	–
2007 Nov 02.9518–Nov 03.2298	N–7	76	2.48	1.62	14.5	64.1	208.9	263.8	–
2007 Nov 03.9632–Nov 03.9825	N–6	6	2.48	1.62	14.3	64.4	207.2	263.5	208
2007 Nov 04.9503–Nov 05.2319	N–5	78	2.48	1.62	14.0	64.7	205.4	263.3	208
2007 Nov 05.9481–Nov 06.2293	N–4	78	2.49	1.62	13.8	65.0	203.6	263.0	208
2007 Nov 13.9258–Nov 14.2159	N+4	76	2.52	1.63	12.2	67.1	186.9	260.8	200
2007 Nov 14.9262–Nov 15.2142	N+5	76	2.52	1.63	12.1	67.4	184.6	260.5	200
2007 Nov 15.9275–Nov 16.2118	N+6	76	2.53	1.63	11.9	67.7	182.3	260.2	200
2007 Nov 16.9254–Nov 17.0383	N+7	30	2.53	1.63	11.8	67.9	179.9	259.9	200
2007 Nov 22.9603–Nov 23.6916	N+13	78	2.55	1.65	11.3	69.5	164.8	258.2	195
2007 Dec 01.9561–Dec 02.1222	N–8	42	2.59	1.70	11.4	71.8	142.2	255.8	177
2007 Dec 02.8300–Dec 03.0240	N–7	60	2.59	1.70	11.5	72.0	140.2	255.6	177

[a]Lunar phase expressed in offset from new Moon ('N') in days.
[b]Number of images obtained.
[c]Heliocentric distance in au.
[d]Geocentric distance in au.
[e]Solar phase angle (Sun-17P-Earth) in degrees.
[f]True anomaly in degrees.
[g]Position angle in degrees east of north of antisolar vector as projected on the sky.
[h]Position angle in degrees east of north of negative velocity vector as projected on the sky.
[i]Position angle in degrees east of north of central axis of the comet's dust tail, whose direction only becomes clearly identifiable in data from 2007 November 3–4 onwards.
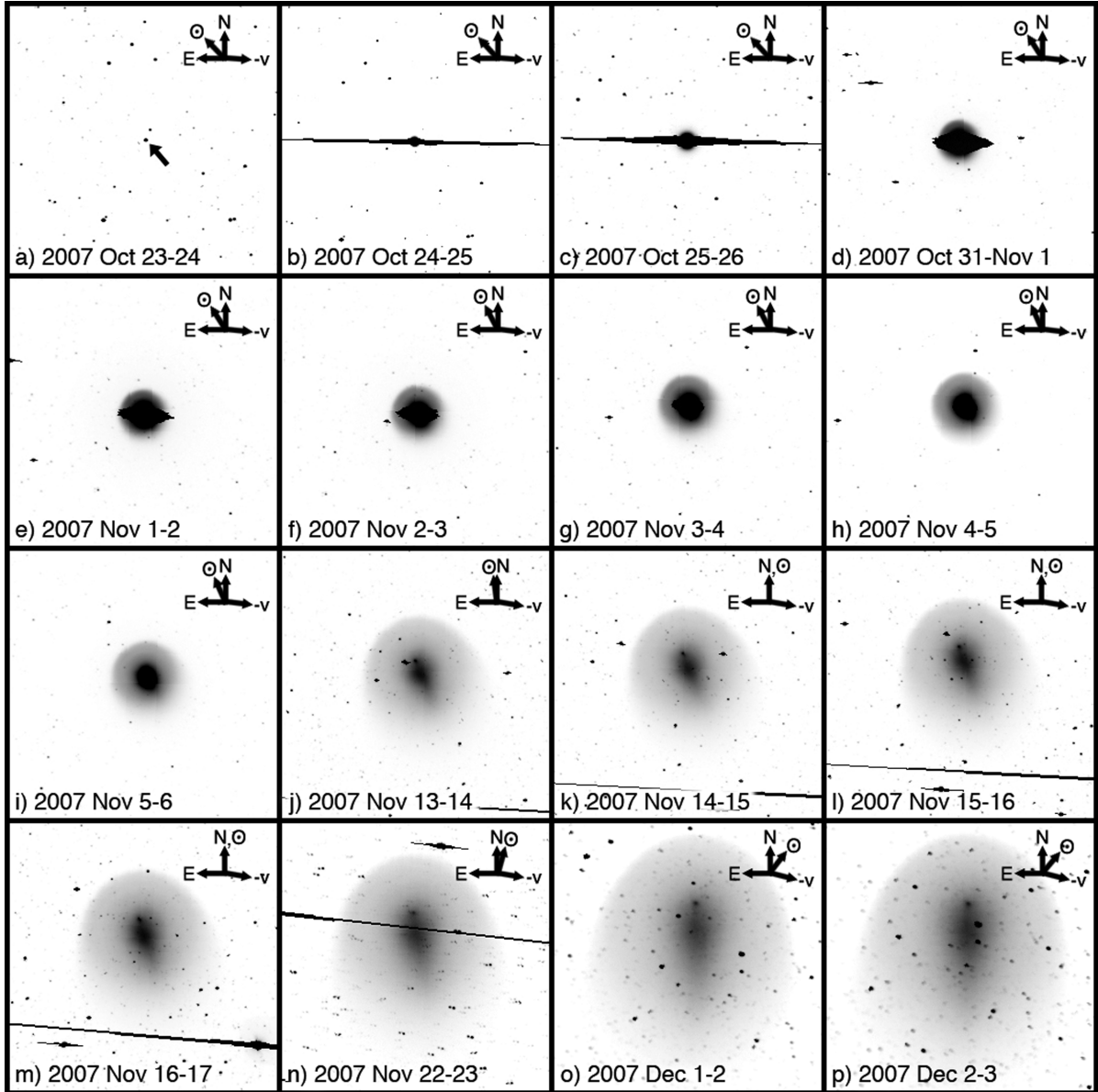
Figure 1. Images of 17P on 16 nights between 2007 October 23 and 2007 December 3 using SuperWASP-N. Each image comprises 30 s of exposure time and is $1° × 1°$ in size. Arrows indicate north (N), east (E), the direction towards the Sun ($\odot$) and the negative heliocentric velocity vector ($-v$). Solid lines intersecting various images are saturated CCD columns from the comet itself or nearby bright field stars.

Table 2. Field stars used for photometry calibration.

Star	R.A.[a]	Dec.[b]	Type[c]	m_V[d]
HIP 16880	03:37:13.97	+49:33:27.12	F6IV-V	10.06
BD+48 965	03:38:51.74	+49:24:18.25	K0	9.05
HIP 16965	03:38:15.41	+51:35:22.47	F4IV	10.32

[a]Right ascension, in hours, minutes and seconds.
[b]Declination, in degrees, arcminutes and arcseconds.
[c]Spectral type.
[d]V-band magnitude.

discussed hereafter is performed using differentially calibrated instrumental fluxes (as described above) unless otherwise specified, and as such is unaffected by uncertainties in these magnitude calibration calculations. All photometry results are shown in Table 3.

3 DATA ANALYSIS

3.1 Light curve

3.1.1 Coma optical depth

If we assume that the coma of 17P is dominated by dust grains and is optically thick on the first night of the comet's outburst (2007 October 23–24), we would expect its brightness (I) to vary linearly with the surface area of the coma as projected on the sky. If the coma radius increases at a linear rate, its surface area will vary as the square of elapsed time, $t - t_0$, since the outburst, giving the following expression for the brightness:

$$I = I_0 + z(t - t_0)^k, \tag{1}$$

where $k = 2$ and z is a scaling constant. Assuming an effective initial brightness, $I_0 \sim 150$ ADU (equivalent to a $\sim 0.05\sigma$ signal in our

Table 3. Nucleus photometry.

UT date	Airmass	Flux[a]	m_V[b]
2007 Oct 23.9851	1.308	1.20 ± 0.07	9.67 ± 0.20
2007 Oct 23.9855	1.306	1.20 ± 0.07	9.66 ± 0.20
2007 Oct 23.9938	1.271	1.29 ± 0.07	9.59 ± 0.20
2007 Oct 23.9942	1.269	1.29 ± 0.07	9.60 ± 0.20
2007 Oct 24.0025	1.237	1.37 ± 0.07	9.53 ± 0.20
2007 Oct 24.0029	1.236	1.38 ± 0.07	9.52 ± 0.20
2007 Oct 24.0113	1.207	1.44 ± 0.07	9.47 ± 0.20
2007 Oct 24.0117	1.206	1.43 ± 0.07	9.48 ± 0.20
2007 Oct 24.0201	1.181	1.53 ± 0.07	9.42 ± 0.20
2007 Oct 24.0205	1.180	1.55 ± 0.07	9.40 ± 0.20
2007 Oct 24.0288	1.158	1.65 ± 0.07	9.34 ± 0.20
2007 Oct 24.0293	1.156	1.65 ± 0.07	9.33 ± 0.20
2007 Oct 24.0366	1.139	1.73 ± 0.07	9.29 ± 0.20
2007 Oct 24.0371	1.138	1.76 ± 0.07	9.27 ± 0.20
2007 Oct 24.0443	1.123	1.83 ± 0.07	9.23 ± 0.20
2007 Oct 24.0448	1.122	1.83 ± 0.07	9.23 ± 0.20
2007 Oct 24.0520	1.109	1.95 ± 0.07	9.16 ± 0.20
2007 Oct 24.0524	1.108	1.95 ± 0.07	9.16 ± 0.20
2007 Oct 24.0597	1.097	2.07 ± 0.07	9.10 ± 0.20
2007 Oct 24.0602	1.096	2.08 ± 0.07	9.10 ± 0.20
2007 Oct 24.0696	1.084	2.27 ± 0.07	9.00 ± 0.20
2007 Oct 24.0701	1.084	2.28 ± 0.07	9.00 ± 0.20
2007 Oct 24.0773	1.076	2.46 ± 0.07	8.91 ± 0.20
2007 Oct 24.0777	1.076	2.48 ± 0.07	8.91 ± 0.20
2007 Oct 24.0850	1.069	2.69 ± 0.07	8.82 ± 0.20
2007 Oct 24.0854	1.069	2.71 ± 0.07	8.81 ± 0.20
2007 Oct 24.0927	1.065	3.00 ± 0.07	8.69 ± 0.20
2007 Oct 24.0931	1.064	2.97 ± 0.07	8.71 ± 0.20
2007 Oct 24.1005	1.061	3.28 ± 0.07	8.60 ± 0.20
2007 Oct 24.1010	1.061	3.29 ± 0.07	8.60 ± 0.20
2007 Oct 24.1093	1.059	3.84 ± 0.07	8.43 ± 0.20
2007 Oct 24.1098	1.059	3.89 ± 0.07	8.42 ± 0.20
2007 Oct 24.1160	1.059	4.21 ± 0.07	8.33 ± 0.20
2007 Oct 24.1164	1.059	4.22 ± 0.07	8.33 ± 0.20
2007 Oct 24.1225	1.060	4.62 ± 0.07	8.23 ± 0.20
2007 Oct 24.1230	1.060	4.68 ± 0.07	8.20 ± 0.20
2007 Oct 24.1292	1.063	5.21 ± 0.07	8.10 ± 0.20
2007 Oct 24.1296	1.063	5.26 ± 0.07	8.10 ± 0.20
2007 Oct 24.1359	1.066	5.88 ± 0.07	7.97 ± 0.20
2007 Oct 24.1364	1.066	6.01 ± 0.07	7.93 ± 0.20
2007 Oct 24.1426	1.071	6.60 ± 0.07	7.80 ± 0.20
2007 Oct 24.1430	1.071	6.65 ± 0.07	7.78 ± 0.20
2007 Oct 24.1492	1.076	7.43 ± 0.07	7.62 ± 0.20
2007 Oct 24.1496	1.077	7.38 ± 0.07	7.64 ± 0.20

[a]Calibrated net flux of comet nucleus in 10^5 ADU.
[b]Approximate equivalent V-band magnitude of comet nucleus.

data), consistent with reported pre-outburst magnitudes of 17P of $m_V \sim 17.0$ (Casali et al. 2007) and fitting only to the first ~2 h of SuperWASP data, we find best-fitting values of $z = 2.3 \times 10^6$ and $t_0 = 2007$ October 23.8 ± 0.1, as reported in Hsieh, Fitzsimmons & Pollacco (2007). This value for t_0 is consistent with the outburst time initially estimated by Gaillard, Lecacheux & Colas (2007).

While this early photometry initially appears to be consistent with a linearly expanding, optically thick coma, combining these data with our analysis of the coma's expansion velocity (described in Section 3.2) shows that this is likely not the case. We can estimate the total scattering cross-section, $A = \pi r_e^2$, of the particles in the coma from

$$p_V r_e^2 = 2.24 \times 10^{22} \times 10^{0.4[\, m_\odot - m(1,1,0)]}, \qquad (2)$$

where p_V is the geometric V-band albedo, assumed here to be $p_V = 0.04$, and $m_\odot = -26.66$ is used for the absolute solar V-band magnitude. Assuming a phase coefficient of $\beta = 0.035$ mag deg^{-1}, we obtain starting and ending absolute magnitudes of $m_{\text{start}}(1, 1, 0) = 6.08$ and $m_{\text{end}}(1, 1, 0) = 5.50$ for the period of observations for which the comet's brightening appears to follow a square law, giving starting and ending total scattering cross-sections of $A_{\text{start}} = 1.41 \times 10^5$ km^2 and $A_{\text{end}} = 2.41 \times 10^5$ km^2. If the coma is optically thick, meaning that the observed scattering cross-section is equal to the total area of the coma, A_{coma}, we obtain starting and ending coma radii of $r_{\text{start}} = 212$ km and $r_{\text{end}} = 277$ km, assuming a circular coma. Our first and last photometry measurements are separated by 6487 s, so the assumption of an optically thick coma yields a coma expansion velocity of only 0.01 km s^{-1}.

This velocity is far slower than our calculated coma expansion velocity and all other reported expansion velocities (cf. Section 3.2). Using a smaller assumed albedo value for the coma dust particles has the effect of increasing the total effective scattering cross-section, therefore increasing the implied expansion velocity. An implausibly low assumed albedo of $p_V = 1.6 \times 10^{-5}$ is required, however, to produce an expansion velocity of 0.5 km s^{-1} (where $r_{\text{start}} = 1.06 \times 10^4$ km and $r_{\text{end}} = 1.38 \times 10^4$ km). Assuming a larger phase coefficient value also increases the implied expansion velocity by increasing the implied brightness of the coma at $\alpha = 0°$, but again, an implausible value for the phase coefficient ($\beta = 0.53$ mag deg^{-1}) is required to produce an expansion velocity of 0.5 km s^{-1}, assuming $p_V = 0.04$. In fact, as shown in Fig. 2, given the range of cometary phase coefficients ($0.01 < \beta < 0.09$; Meech & Jewitt 1987; Snodgrass, Lowry & Fitzsimmons 2008) and albedos ($0.01 < p_V < 0.07$; Lamy et al. 2004) measured to date, no plausible combination of β and p_V is able to account for our photometry data given the assumption of an optically thick coma with an outer edge expanding at 0.5 km s^{-1}.

The implausible conditions necessary for 17P's coma to be optically thick strongly suggest that the coma is optically thin even in our earliest observations of the outburst, confirming the results of Sekanina (2009a). This conclusion is supported by our coma expansion analysis (Section 3.2) which suggests that the radius of the outer edge of the coma should have already been 5.0×10^4 km at the time of SuperWASP's first image of the comet on the first night of the outburst, making it approximately 200 times larger than an optically thick coma would be (assuming typical cometary albedo and phase coefficient values of $p_V = 0.04$ and $\beta = 0.035$ mag deg^{-1}). We therefore find that the rapid brightening we observed for the comet on 2007 October 23–24 must have been caused by a process other than the expansion of an optically thick coma.

3.1.2 Evidence for fragmentation

If we assume that 17P's coma was already optically thin by the time of our first observation, it is possible that most of the observed material could have been emitted on a very short time-scale around the time of the outburst, and that the brightening of the coma was primarily due to the fragmentation of the dust grains into smaller particles leading to an increase in reflecting surface area. This scenario was also suggested by Gaillard et al. (2007) and Kobayashi et al. (2007). Fragmentation of dust particles has also been inferred from *in situ* measurements at other comets such as 1P/Halley (Ho et al. 2007) and 81P/Wild 2 (Tuzzolino et al. 2004), as well as
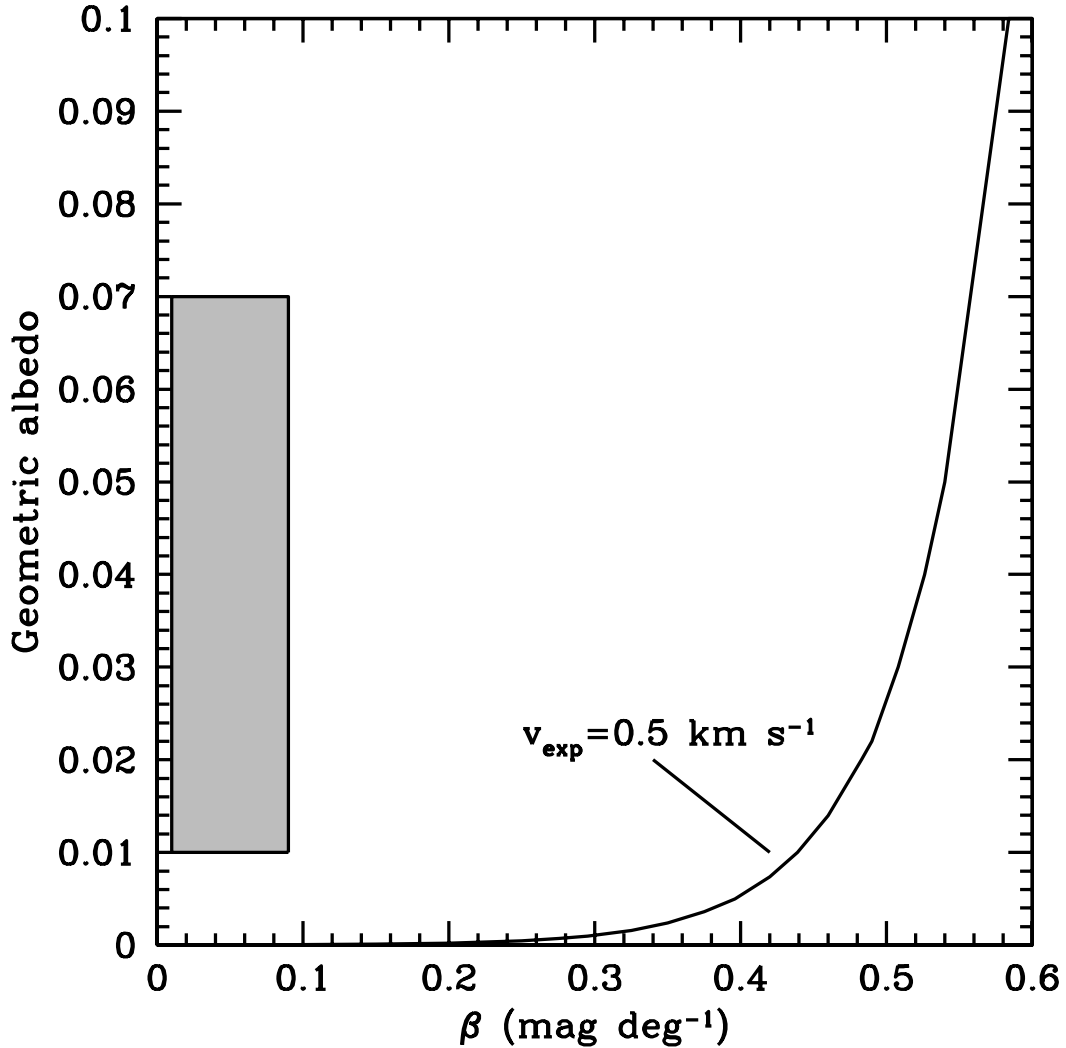
Figure 2. The locus of values (plotted as a solid line) of β and albedo required for the particles in an optically thick coma with an outer edge expanding at 0.5 km s^{-1} in order to account for the observed light curve in Fig. 3. The shaded area indicates the range of cometary β and albedo values measured to date.

many ground-based observations of comets such as C/Hale-Bopp (Pittichová et al. 1997).

If a dust grain breaks into two daughter grains when it fragments, the original visible cross-sectional area of the dust increases by a factor f. As long as the fragmentation time-scale, t_{frag}, and the albedo are roughly size-invariant (i.e. they do not change as fragmentation progresses), the dust's total visible cross-section, and hence its brightness, will increase exponentially with the form

$$I(t - t_0) = I_0 e^{z(t-t_0)} \equiv I_0 f^{(t/t_{frag})}, \qquad (3)$$

where I_0 is the brightness of the dust at an initial time t_0. The dust grain fragmentation time-scale t_{frag} is related by the brightness exponent z by

$$t_{frag} = \frac{\ln f}{z}. \qquad (4)$$

For splitting into two daughter fragments, the maximum value of f is when the daughter grains have equal mass, giving $f(\text{max}) = 1.26$. For splitting into more than two daughter fragments, t_{frag} will be larger by a factor $1.44 \ln N$, where N is the number of simultaneously produced daughter particles and we assume that all daughter particles have equal mass.

Analysing our data in the context of this fragmentation model, we fit 17P's early light curve to the following function:

$$I = A[e^{z(t-t_0)} - 1] + I_0. \qquad (5)$$

Mathematically, A and t_0 in this function cannot be fit simultaneously, meaning that equation (5) cannot be used to derive a unique outburst time. Thus, for this analysis, we assume an outburst time of $t_0 = 2007$ October 23.3 as determined from the expansion of the coma (discussed below in Section 3.2). Fitting the entire $\sim$4 h of unsaturated 17P data, we find best-fitting parameters of $A = (1.0 \pm 0.2) \times 10^{-2}$ ADU, $z = 21.2 \pm 0.2$ d^{-1} and $I_0 = (1.10 \pm 0.02) \times 10^5$ ADU (corresponding to $m_V \sim 9.8$ mag). An exponential function using these best-fitting parameters (where fluxes have been converted to equivalent V-band magnitudes), along with the square law discussed above, is plotted in Fig. 3.

Overlaying on Fig. 3 other published photometry (Table 4) from the Spanish Meteor and Fireball Network (SPMN; Trigo-Rodriguez et al. 2008), and from J. A. Henríquez Santana and G. Muler (Sposetti et al. 2007), we find slight discrepancies between our computed magnitudes and these other data. However given the unspecified calibration methods of Henríquez Santana and Muler and the uncertain absolute calibration of both SuperWASP and SPMN
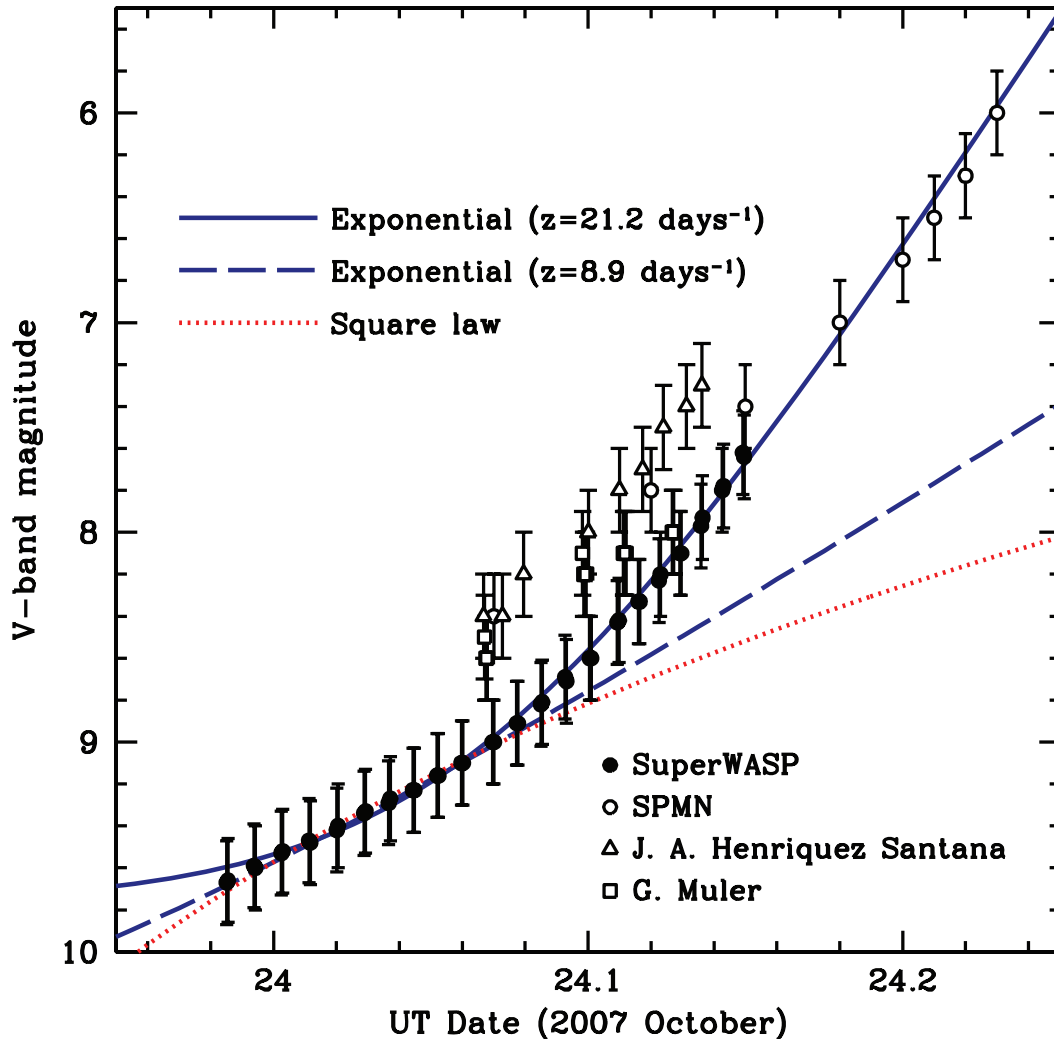
Figure 3. *V*-band magnitudes (solid circles) measured for the nucleus of 17P with the best-fitting square-law function and best-fitting exponential function plotted as a dashed line and a solid line, respectively.

data (stemming from the use of non-standard filters at both facilities), we judge our data and our derived best-fitting exponential brightening function to be approximately consistent with these other data.

This result implies that dust particles in 17P's coma had average fragmentation lifetimes of $t_{\rm frag} \lesssim 10^3$ s, assuming bilateral splitting. However, we note that when fitting this exponential function to our data, the fit is noticeably poorer to the first half of the data set compared to the second half. Functionally, this discrepancy can be accounted for if z increases over our observing period. In Fig. 3, a second exponential function is also shown fitted only to the first 2 h of data with $z = 8.9$ d^{-1}, $t_0 = 2007$ October 23.3, $A = 200$ ADU and $I_0 = 3.0 \times 10^4$ ADU corresponding to $m_V \sim 11.2$ mag. This gives a fragmentation time-scale (assuming two daughter grains per splitting event) of $t_{\rm frag} \lesssim 2 \times 10^3$ s. The improved accuracy of such a two-exponential fit implies that as the outburst progressed, the rate of fragmentation increased. This behaviour could physically correspond to a situation in which the outburst ejected clumps of dust bound together by ice. As the ice sublimated and became progressively unable to bind those clumps together, increasingly rapid disintegration could have followed.

3.2 Coma expansion

Using data taken from 2007 October 31 onwards (when at least a portion of the coma had expanded beyond the central saturated core of the comet in our data), we can measure the size of the dust coma on successive nights and thus determine its expansion rate and, in principle, the time of the outburst's onset. Two complications in this method as noted by Sekanina (2008a) are the presence of an extended gas coma with poorly defined edges that obscures the extent of the relatively more well-defined dust coma (cf. Section 3.6), and the non-sphericity of the coma after approximately 2007 November 3.

Additionally, we note that as the coma expands and fades, successive portions of the outer coma are rendered unobservable as they approach the signal-to-noise ratio detection limit of the background sky. This process complicates measurements of the size and expansion rate of the coma since it means that the visually determined 'edge' of the coma does not correspond to the same parcels of coma dust at all times, but instead simply represents the locus of points at which the coma's surface brightness is detectable against the sky. Even assuming the sky brightness to be approximately constant from night to night (which it is not, due to the changing proximity

Table 4. Selected photometry from other observers.

UT date	Mag.	Obs.[a]	Reference
2007 Oct 24.066 82	8.4	J51	Sposetti et al. (2007)
2007 Oct 24.067 08	8.5	J47	Sposetti et al. (2007)
2007 Oct 24.067 50	8.6	J47	Sposetti et al. (2007)
2007 Oct 24.067 91	8.6	J47	Sposetti et al. (2007)
2007 Oct 24.07	8.4	SPMN	Trigo-Rodríguez et al. (2008)
2007 Oct 24.072 82	8.4	J51	Sposetti et al. (2007)
2007 Oct 24.079 56	8.2	J51	Sposetti et al. (2007)
2007 Oct 24.098 23	8.1	J47	Sposetti et al. (2007)
2007 Oct 24.098 64	8.2	J47	Sposetti et al. (2007)
2007 Oct 24.099 43	8.2	J47	Sposetti et al. (2007)
2007 Oct 24.100 07	8.0	J51	Sposetti et al. (2007)
2007 Oct 24.109 94	7.8	J51	Sposetti et al. (2007)
2007 Oct 24.111 26	8.1	J47	Sposetti et al. (2007)
2007 Oct 24.111 66	8.1	J47	Sposetti et al. (2007)
2007 Oct 24.112 05	8.1	J47	Sposetti et al. (2007)
2007 Oct 24.117 35	7.7	J51	Sposetti et al. (2007)
2007 Oct 24.12	7.8	SPMN	Trigo-Rodríguez et al. (2008)
2007 Oct 24.123 98	7.5	J51	Sposetti et al. (2007)
2007 Oct 24.126 80	8.0	J47	Sposetti et al. (2007)
2007 Oct 24.127 19	8.0	J47	Sposetti et al. (2007)
2007 Oct 24.131 31	7.4	J51	Sposetti et al. (2007)
2007 Oct 24.136 19	7.3	J51	Sposetti et al. (2007)
2007 Oct 24.15	7.4	SPMN	Trigo-Rodriguez et al. (2008)
2007 Oct 24.18	7.0	SPMN	Trigo-Rodriguez et al. (2008)
2007 Oct 24.20	6.7	SPMN	Trigo-Rodriguez et al. (2008)
2007 Oct 24.21	6.5	SPMN	Trigo-Rodriguez et al. (2008)
2007 Oct 24.22	6.3	SPMN	Trigo-Rodriguez et al. (2008)
2007 Oct 24.23	6.0	SPMN	Trigo-Rodriguez et al. (2008)

[a]Observatory: J47: Observatorio Nazaret (G. Muler), 0.20-m + CCD; J51: Observatorio Atlante, Tenerife (J. A. Henríquez), 0.2-m + CCD; SPMN: Spanish Meteor and Fireball Network.

and phase of the Moon and the altitude of observation), since the surface brightness of a given parcel of dust decreases as the coma expands and becomes more diffuse, following a point of constant brightness will actually lead steadily inwards in the expanding reference frame of the coma. Thus, over time, simply measuring the coma's observable edge will lead to increasing underestimates of the coma's true size, leading to an underestimate of its true expansion velocity.

With these concerns in mind, we prepare our data for the measurement of the coma size and expansion rate by rotating comet images from each night to align the central axis (as projected in the image plane) of the comet's elongated coma with each image's vertical axis. This procedure is a straightforward matter for data obtained on 2007 November 13 onwards, in which the coma is visibly elongated, and the position angle of the central axis is clear (Table 1). For data obtained on 2007 November 6 or earlier, the coma is largely circular, making it difficult to discern the orientation of its central axis. For these data, we simply adopt the antisolar vector (as projected in the plane of the sky) as the coma's central axis, and apply image rotations accordingly.

For each rotated image, we measure the flux in the coma along a horizontal three-pixel-wide strip passing through the comet nucleus, where the nucleus is assumed to be at the centre of the nearly circular coma in data obtained prior to 2007 November 5–6. We then average the fluxes contained in pairs of pixels which are equidistant from the nucleus on each side of that axis. Finally, we normalize the results to the flux of the photometry aperture centred on the nucleus and plot these normalized fluxes as a function of distance

from the comet's nucleus for each image (Fig. 4). By constructing profiles in this way, we aim to minimize the effects on our results of the coma's non-sphericity and highly projected orientation in the sky.

We note immediately that the surface brightness profiles we obtain are of approximately the same form from night to night (with the exception of the profile on 2007 November 22–23 whose anomalous appearance we attribute to the close proximity of the nearly full moon on that night). This stability of our surface brightness profiles gives us confidence that we are able to achieve consistent results despite the large spatial scale of the coma and widely varying stellar backgrounds. Significantly, we also note that these linear surface brightness profiles do not match the r^{-1} radial surface brightness profile of a canonical spherically symmetric, steady-state cometary dust coma. Instead, profiles from 2007 October 31–November 1 to 2007 November 5–6 (Figs 4a–f) consist of saturated pixels near the nucleus, followed by a region of moderate slope ($\sim r^{-0.6}$ to $r^{-0.9}$, hereafter 'Region 1') leading into an extremely steep section ($\sim r^{-5}$ to r^{-11}, hereafter 'Region 2'). Region 2 then transitions into another region of moderate slope ($\sim r^{-0.7}$ to $r^{-0.9}$, hereafter 'Region 3') which finally becomes essentially horizontal ($\sim r^{0.0}$, hereafter 'Region 4') far from the nucleus where the surface brightness profile becomes dominated by the background sky. For data from 2007 November 13–14 onwards (Figs 3g–m), the central portion of the coma is no longer saturated, while Region 2 of each profile transitions directly into Region 4 without passing through Region 3. Where possible, we compute best-fitting linear functions for each of these regions in each profile (Fig. 4, Table 5). Region 1 parameters are not calculated for 2007 October 31–November 3 due to extensive inner coma saturation on these dates.

The observed evolution of 17P's coma profile is consistent with a growing coma which maintains an approximately constant morphology as it expands and fades. We interpret Region 1 as the dust-dominated portion of the coma, and Region 2 as the edge of the dust coma, with its steep slope likely indicating a sharp cut-off at the small end of the size distribution of visible grains. The inconsistency with the slope of Region 1 (-0.9, declining to -0.6) with that of a canonical steady-state dust coma under radiation pressure (-1.0 to -1.5) indicates that the coma is not in fact steady-state. Such a steadily decreasing slope would in fact be expected if a single outburst is assumed to account for the majority of the observed dust coma, as faster, smaller dust grains in the outer coma will expand at a higher velocity than slower-moving, large particles in the inner coma. We hypothesize that the transient Region 3 could be due to gas extending beyond the outermost edge of the dust that otherwise dominates the coma profile. We discuss this hypothesis at length below (Section 3.6). The fluctuating length of Region 2 after the disappearance of Region 3 confirms our concern that the intersection of the outer coma and the sky is an unreliable determinant of coma size.

With the above issues in mind, we suggest that a more precise measure of the expansion rate of 17P's coma can be achieved by tracking the motion of reference points *within* the coma. Specifically, we suggest that the relatively well-defined transitions between the various surface brightness profile regions described above could be useful reference points. We note that uncertainty is not entirely eliminated by the use of this method as the shape of the coma profile does evolve slightly over time (cf. Table 5) meaning that our chosen reference points likely shift slightly within the expanding reference frame of the coma. None the less, given the fundamentally problematic nature described above of measuring the expansion of a progressively fading coma using brightness-dependent reference
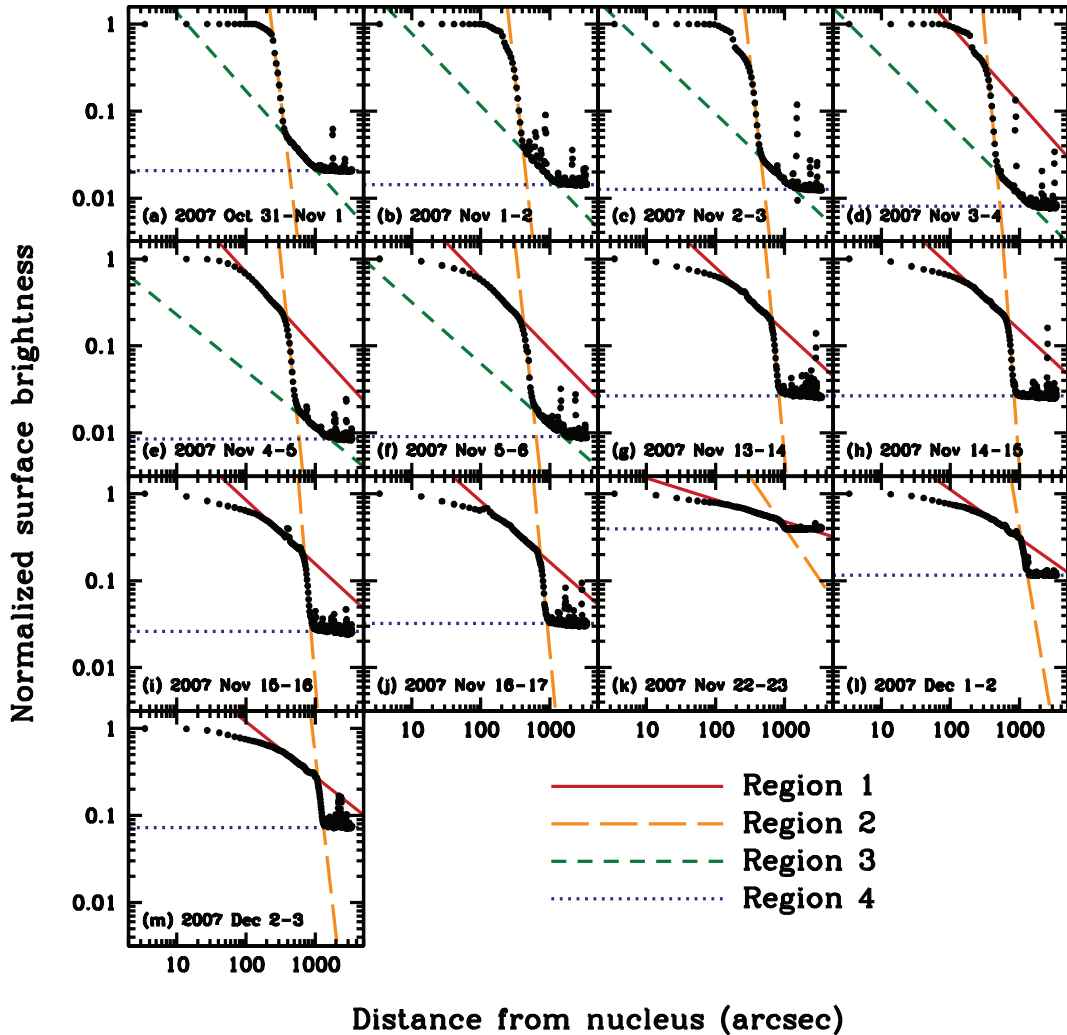
Figure 4. Linear surface brightness profiles of the coma of 17P as measured along a line passing through the nucleus and perpendicular to the coma's central axis, taken to be the antisolar vector (as projected in the sky) for (a)–(f) and the coma's axis of symmetry for (g)–(m). Measured normalized surface brightness values are plotted as solid dots, while linear fits to Regions 1, 2, 3 and 4 of each surface brightness profile (as described in the text) are plotted as solid lines, large-dashed lines, small-dashed lines, and dotted lines, respectively. Region 1 parameters are not calculated for October 31–November 3 due to extensive inner coma saturation on these dates. Region 3 is absent for November 13–14 onwards. We note that with the exception of November 22–23 when the Moon was nearly full, the sky brightness is relatively constant (Table 5. The apparent increase in Region 4 over time is due to the decrease in peak coma brightness, to which each surface brightness profile is individually normalized.

points, we believe tracking morphology-dependent reference points to be the most reliable method at our disposal.

We define the transition point between two regions of the coma's surface brightness profile as the intersection of the best-fitting linear functions (in log–log space) of those regions. As we seek to avoid being affected by fluctuations in sky brightnesses and the steady fading of the outer coma, we first only concern ourselves with the positions of the intersections of Regions 1 and 2 and Regions 2 and 3 (Table 6), ignoring intersections of those regions with Region 4 (the sky). Plotting the distances of these intersection points from the nucleus as a function of time (Fig. 5), we find best-fitting linear solutions corresponding to an expansion velocity of $v_{exp} = 0.41 \pm 0.02\,\mathrm{km\ s^{-1}}$ and a start date of $t_0(1-2) = 2007$ October 23.3 ± 0.3 (very close to the time of the final SuperWASP observation of the comet on the night prior to the outburst's discovery) for the intersection point between Regions 1 and 2. An expansion velocity of $v_{exp} = 0.55 \pm 0.02\,\mathrm{km\ s^{-1}}$ and a start date of $t_0(2-3) = 2007$ October 23.1 ± 0.3 is found for the intersection

point between Regions 2 and 3. The latter expansion rate is consistent with previously reported values (e.g. Gaillard et al. 2007; Snodgrass et al. 2007; Lin et al. 2009) We believe $t_0(1-2)$ to be the more reliable extrapolated value as it is derived using a reference point within the dust coma itself. By contrast, $t_0(2-3)$ is derived using the intersection of the dust-dominated and gas-dominated components of the coma.

For the solution for the outburst time using the intersection between Regions 1 and 2, we use data up to November 17 only. Beyond this date, the location of this reference point within the expanding frame of the coma appears to have shifted as expected (discussed above), and as such, we omit these data in this portion of our analysis.

For completeness, we also consider the intersections of Region 2 and Region 3 with the sky (Region 4). Plotting the distances of these points (Table 6) as a function of time and omitting data points from 2007 October 31–November 1 (due to the moderately high sky background on that night) and from 2007 November

Table 5. Best-fitting linear parameters for normalized surface brightness profiles.

UT date	Sky[a] level	Region 1[b] m	b	Region 2[c] m	b	Region 3[d] m	b	Region 4[e] m	b
2007 Nov 01.089 78	2.1 ± 0.1	–	–	-6.5 ± 0.2	15.5 ± 0.2	-0.9 ± 0.1	1.0 ± 0.1	(0.0)	-1.7 ± 0.1
2007 Nov 02.170 89	1.6 ± 0.1	–	–	-7.1 ± 0.2	17.1 ± 0.2	-0.8 ± 0.1	0.7 ± 0.1	(0.0)	-1.8 ± 0.1
2007 Nov 03.147 26	1.4 ± 0.1	–	–	-7.1 ± 0.2	17.3 ± 0.2	-0.8 ± 0.1	0.5 ± 0.1	(0.0)	-1.9 ± 0.1
2007 Nov 03.973 23	0.8 ± 0.1	-0.9 ± 0.1	1.8 ± 0.1	-9.1 ± 0.2	22.7 ± 0.2	-0.8 ± 0.1	0.4 ± 0.1	(0.0)	-2.1 ± 0.1
2007 Nov 05.139 39	0.9 ± 0.1	-0.9 ± 0.1	1.6 ± 0.1	-7.7 ± 0.2	19.2 ± 0.2	-0.7 ± 0.1	0.0 ± 0.1	(0.0)	-2.1 ± 0.1
2007 Nov 06.056 27	0.8 ± 0.1	-0.8 ± 0.1	1.4 ± 0.1	-7.2 ± 0.2	18.1 ± 0.2	-0.7 ± 0.1	0.2 ± 0.1	(0.0)	-2.1 ± 0.1
2007 Nov 14.025 72	1.1 ± 0.1	-0.7 ± 0.1	1.4 ± 0.1	-8.6 ± 0.2	23.5 ± 0.2	–	–	(0.0)	-1.6 ± 0.1
2007 Nov 15.126 98	1.0 ± 0.1	-0.7 ± 0.1	1.4 ± 0.1	-10.6 ± 0.2	29.3 ± 0.2	–	–	(0.0)	-1.6 ± 0.1
2007 Nov 16.211 82	0.9 ± 0.1	-0.7 ± 0.1	1.4 ± 0.1	-9.4 ± 0.2	26.2 ± 0.2	–	–	(0.0)	-1.6 ± 0.1
2007 Nov 16.961 57	1.1 ± 0.1	-0.7 ± 0.1	1.3 ± 0.1	-8.3 ± 0.2	23.2 ± 0.2	–	–	(0.0)	-1.5 ± 0.1
2007 Nov 23.130 81	12.8 ± 0.1	-0.3 ± 0.1	0.4 ± 0.1	-1.2 ± 0.2	3.2 ± 0.2	–	–	(0.0)	-0.4 ± 0.1
2007 Dec 02.122 17	1.2 ± 0.1	-0.6 ± 0.1	1.2 ± 0.1	-4.7 ± 0.2	13.6 ± 0.2	–	–	(0.0)	-0.9 ± 0.1
2007 Dec 03.023 99	0.7 ± 0.1	-0.6 ± 0.1	1.3 ± 0.1	-6.9 ± 0.2	20.3 ± 0.2	–	–	(0.0)	-1.1 ± 0.1

[a]Average surface brightness of background sky in ADU arcsec^{-2}.

[b]Best-fitting parameters for Region 1 of surface brightness profiles in Fig. 4 using $y = mx + b$ in log–log space, where parameters for October 31–November 3 are not calculated due to extensive inner coma saturation on these dates, and estimated uncertainties are dominated by variations in measured coma morphology from image to image during individual nights due to small sky brightness changes and field star interference.

[c]Best-fitting parameters for Region 2, where estimated uncertainties are dominated by coma morphology variations during individual nights.

[d]Best-fitting parameters for Region 3, where parameters for November 14–December 3 are not calculated due to the absence of this profile region on these dates, and estimated uncertainties are dominated by coma morphology variations during individual nights.

[e]Best-fitting parameters for Region 4, where $m = 0.0$ is assumed, and estimated uncertainties are dominated by coma morphology variations during individual nights.

Table 6. Coma size measurements.

UT date	JD 245 0000.5	km arcsec$^{-1,a}$	R1–R2 Distance[b]	R2–R3 Distance[c]	R3–R4 Distance[d]	R2–R4 Distance[e]
2007 Nov 01.089 78	4405.089 78	1178.1	–	4.3 ± 0.3	12.3 ± 0.3	5.0 ± 0.3
2007 Nov 02.170 89	4406.170 89	1178.1	–	4.9 ± 0.3	14.7 ± 0.3	5.5 ± 0.3
2007 Nov 03.147 26	4407.147 26	1178.1	–	5.3 ± 0.3	16.2 ± 0.3	6.0 ± 0.3
2007 Nov 03.973 23	4407.973 23	1178.1	4.2 ± 0.3	5.6 ± 0.3	17.3 ± 0.3	6.2 ± 0.3
2007 Nov 05.139 39	4409.139 39	1178.1	4.6 ± 0.3	6.3 ± 0.3	19.3 ± 0.3	6.9 ± 0.3
2007 Nov 06.056 27	4410.056 27	1178.1	4.8 ± 0.3	6.7 ± 0.3	18.7 ± 0.3	7.1 ± 0.3
2007 Nov 14.025 72	4418.025 72	1185.4	7.8 ± 0.3	–	–	9.8 ± 0.3
2007 Nov 15.126 98	4419.126 98	1185.4	8.2 ± 0.3	–	–	10.0 ± 0.3
2007 Nov 16.211 82	4420.211 82	1185.4	8.5 ± 0.3	–	–	10.5 ± 0.3
2007 Nov 16.961 57	4420.961 57	1185.4	8.6 ± 0.3	–	–	10.8 ± 0.3
2007 Nov 23.130 81	4427.130 81	1199.9	10.2 ± 0.3	–	–	12.4 ± 0.3
2007 Dec 02.122 17	4436.122 17	1236.3	13.1 ± 0.3	–	–	16.1 ± 0.3
2007 Dec 03.023 99	4437.023 99	1236.3	13.6 ± 0.3	–	–	16.4 ± 0.3

[a]Conversion factor used to compute physical distances at geocentric distance of the comet from angular distances.

[b]Distance from nucleus of intersection point between Regions 1 and 2 of linear surface brightness profiles in 10^5 km, where distances on October 31–November 3 are not calculated due to the unavailability of Region 1 parameters due to extensive inner coma saturation on these dates.

[c]Distance from nucleus of intersection point between Regions 2 and 3 in 10^5 km.

[d]Distance from nucleus of intersection point between Regions 2 and 4x in 10^5 km, where distances on November 14–December 3 are not calculated due to the absence of Region 2 on these dates.

[e]Distance from nucleus of intersection point between Regions 3 and 4 in 10^5 km.

5–6 onwards (due to the notable deviation of points from those nights from the trend exhibited by points prior to 2007 November 5–6), we find best-fitting linear solutions corresponding to an expansion velocity of $v_{exp} = 1.7 \pm 0.1$ km s^{-1} and a start date of $t_0(2-4) =$ 2007 October 22.8 ± 0.5 for the intersection point between Region 2 and the sky. For the intersection point between Region 3 and the sky we measure an expansion velocity of $v_{exp} = 0.4 \pm 0.1$ km s^{-1} and a start date of $t_0(3-4) =$ 2007 October 17.6 ± 0.5. These derived expansion start dates for these reference points are significantly ear-

lier than plausible from reported observations, which is the expected result of using a method that underestimates the coma's expansion velocity.

3.3 Kinematic structure of the Coma

In Section 3.2, we find that outburst times, $t_0(1-2)$ and $t_0(2-3)$, as derived from tracking material at two different locations in 17P's outer coma were coincident, strongly suggesting that this part of
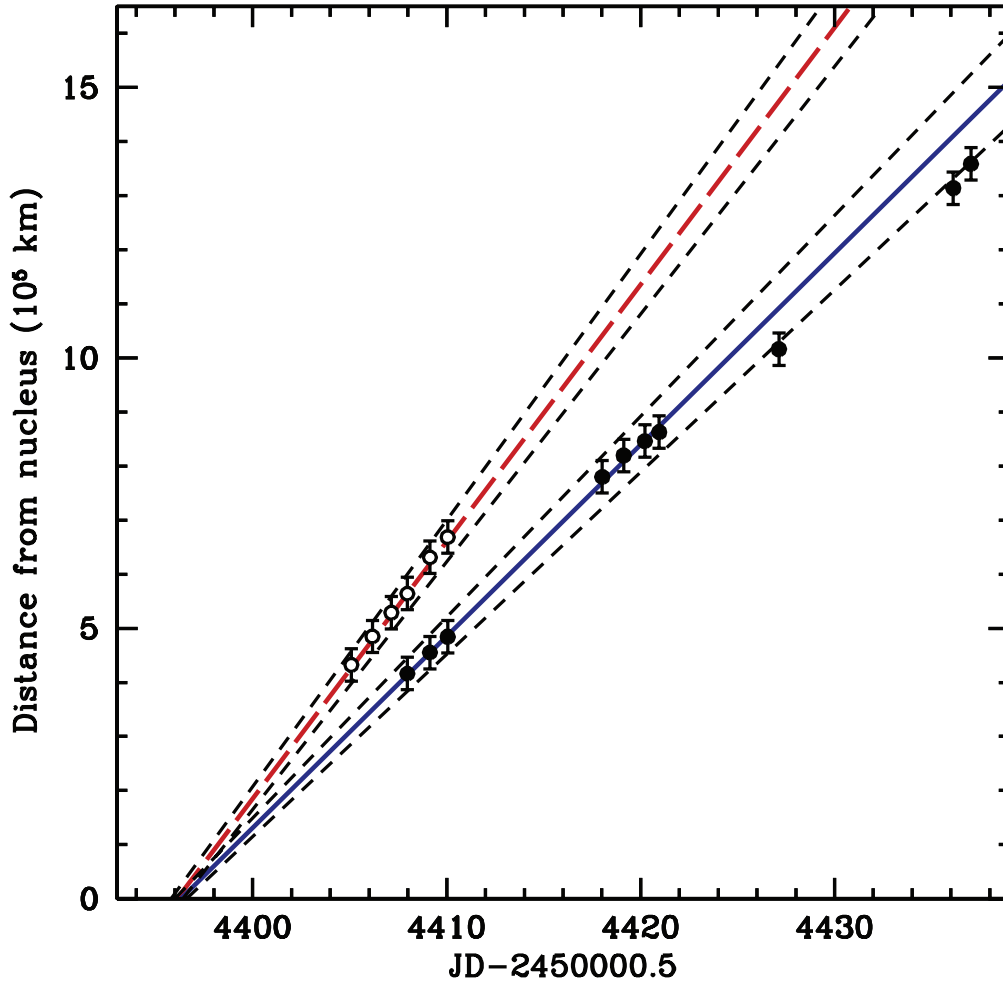
Figure 5. Distances from the nucleus to the intersection points of Regions 1 and 2 (solid circles) and Regions 2 and 3 (open circles) of the linear surface brightness profiles of 17P's coma, as described in the text, between 2007 October 31 and November 1 and 2007 December 2–3 (where JD 245 0000.5 = 4400.0 corresponds to 2007 October 27.0). The best-fitting linear function following the movement of the first intersection point is shown as a solid line, while the best-fitting linear function following the movement of the second intersection point is shown as a large-dashed line. The last three intersection points of Regions 1 and 2 are plotted for reference but are not included in the fit as explained in Section 3.2. Small-dashed lines indicate the range of linear fits permitted by the parameter uncertainties we report for the best-fitting functions.

the coma is dominated by material ejected in a near-instantaneous explosive manner, rather than over an extended period of time. Specifically, by fitting the projected velocity v_{exp} of material in the outer coma at a given projected distance r from the nucleus on a given date t, we find the following relationship:

$$v_{exp} = 0.95 \frac{r}{t - t_0} \pm 0.02 \text{ km s}^{-1}. \tag{6}$$

This velocity gradient is most likely a particle size effect, where smaller particles have larger velocities imparted to them by gas drag during their initial ejection due to their smaller ratio of mass to surface area. The observed projected velocity of an ejected dust particle also depends on the angle of its ejection from the nucleus with respect to the plane of the sky, where dust particles with velocity vectors perpendicular to the line of sight (i.e. parallel to the plane of the sky) will have the greatest apparent velocities. Thus, while all material observed at a given point in the coma is moving at the same projected velocity from the nucleus, that material actually consists of a range of highly projected, small, fast-moving particles, and less-projected, larger, more slowly moving particles. These particles are additionally affected by solar radiation pressure

which eventually causes particles having identical projected ejection velocities but different sizes to diverge, as can be seen by the evolution of the shape of 17P's coma profile (cf. Table 5; Fig. 4). Given the large ejection speeds of particles in the outer coma relative to the acceleration due to solar radiation, the overall effect remains relatively small over the short time interval that we consider here.

Given the low spatial resolution and saturation in much of our SuperWASP data, we are unable to probe the comet's inner coma in sufficient detail to rule out the possibility of later emission from the nucleus. Montalto et al. (2008) did however perform an analysis of the inner coma, fitting a bi-dimensional Gaussian to the innermost portion of the dust cloud (∼30 arcsec), centred on the dust cloud's brightness peak (instead of on the nucleus as in our analysis), and plotting the mean of the σ_x and σ_y of their best-fitting solutions as a function of JD. They derived an average expansion velocity of $v_{exp} = 0.200 \pm 0.004 \text{ km s}^{-1}$ for material located approximately 1.05×10^5 km from the cloud centre on 2007 November 02, and a radial velocity gradient of $v_{exp} = r \, (0.3 \pm 0.2) \times 10^{-5} \text{ s}^{-1}$ on the same date. Given the stated uncertainties, their derived velocity gradient is consistent with the velocity gradient we expect from

equation (6) [$v_{exp} = r\,(0.13 \pm 0.02) \times 10^{-5}\,\mathrm{s^{-1}}$], although their derived velocity ($v_{exp} = 0.200 \pm 0.004\,\mathrm{km\,s^{-1}}$) for material at 1.05×10^{5} km from the cloud centre is not consistent ($v_{exp} = 0.14 \pm 0.02\,\mathrm{km\,s^{-1}}$, according to equation 6).

The large plate scale of SuperWASP's CCDs means that we cannot probe the central 30 arcsec of 17P's coma. Beyond this distance, the coma deviates significantly from a Gaussian profile (as also noted by Montalto et al. 2008). As such, we are unable to repeat and verify the analysis described above using our data. We do note, however, that the large amount of scatter in their data and the lack of actual convergence at a single start time of their plots showing the expansion of the coma in four different filters suggests that their value for the velocity gradient in the inner coma may be unreliable. We also note that their computed expansion velocity and extrapolation of their coma expansion plots imply ejection of the material on 2007 October 27.0 ± 0.7, significantly later than the actual observed start of the outburst on the night of 2007 October 23–24. This large discrepancy between implied ejection times, even accounting for uncertainties, strongly suggests that the material in the inner coma at the time of their observations was not in fact ejected during the initial outburst. In turn, this suggests the existence of some continued emission from the nucleus as late as 2.5 d following the initial outburst.

3.4 The 'false nucleus'

As noted by many observers of 17P, the comet's coma actually exhibited two brightness peaks, one of which was the comet's nucleus and another which we hereafter refer to as the 'false nucleus'. This second brightness peak was also referred to in observation reports as a 'chunk' or 'blob', and was hypothesized by some to be due to a large nuclear fragment that had detached from the primary comet nucleus and was slowly drifting away (e.g. Drahus et al. 2007; Snodgrass et al. 2007; Trigo-Rodriguez et al. 2007). Arai et al. (using data from 2007 October 27 and 30) and Montalto et al. (using data from 2007 October 27 and 31), measured projected drift velocities of 150 and 127 m s^{-1}, respectively (Trigo-Rodriguez et al. 2007). Montalto et al. additionally derived a separation time of 2007 October 25.6 ± 0.2, and later reported a revised drift velocity of $135 \pm 1\,\mathrm{m\,s^{-1}}$ (Montalto et al. 2008). Subsequent analysis of 17P images by investigators such as Lecacheux et al. (in Trigo-Rodriguez et al. 2007), Stevenson, Kleyna & Jewitt (2010) and Reach et al. (2010) revealed the false nucleus to be concentrations of material in a series of dust trails receding from the nucleus.

To test reported velocity measurements of the densest concentration of material in these dust trails, we measure projected distances between the true nucleus and false nucleus in our own data taken between 2007 November 5 and 2007 December 3 (Table 7) and plot these as a function of time (Fig. 6). Assuming a constant drift velocity, we find a best-fitting projected linear velocity of $v_{drift} = 120 \pm 5\,\mathrm{m\,s^{-1}}$ and an initial separation time of $t_{sep} = 2007$ October 23.9 ± 0.5, roughly consistent with other derived outburst times. The estimated uncertainties primarily reflect the difficulty of precisely determining the position of the rather ill-defined false nucleus on each night.

3.5 Dust modelling

One key to understanding the nature of 17P's outburst is determining whether the comet's nucleus is a plausible primary emission source, as we have assumed thus far, or if the coma could be dominated by dust ejected from another source, perhaps a separated fragment

Table 7. False nucleus distance measurements.

UT date	JD 245 0000.5	Sep. dist.[a] arcsec	Sep. dist.[a] 10^5 km
2007 Nov 13.925 76	4417.925 76	186 ± 7	2.2 ± 0.1
2007 Nov 14.025 72	4418.025 72	184 ± 7	2.2 ± 0.1
2007 Nov 14.111 86	4418.111 86	189 ± 7	2.2 ± 0.1
2007 Nov 14.215 86	4418.215 86	182 ± 7	2.2 ± 0.1
2007 Nov 14.926 19	4418.926 19	200 ± 7	2.4 ± 0.1
2007 Nov 15.019 77	4419.019 77	182 ± 7	2.2 ± 0.1
2007 Nov 15.126 98	4419.126 98	199 ± 7	2.4 ± 0.1
2007 Nov 15.214 17	4419.214 17	199 ± 7	2.4 ± 0.1
2007 Nov 15.927 46	4419.927 46	201 ± 7	2.4 ± 0.1
2007 Nov 16.023 21	4420.023 21	206 ± 7	2.4 ± 0.1
2007 Nov 16.116 63	4420.116 63	199 ± 7	2.4 ± 0.1
2007 Nov 16.211 83	4420.211 83	203 ± 7	2.4 ± 0.1
2007 Nov 16.925 35	4420.925 35	214 ± 7	2.5 ± 0.1
2007 Nov 16.961 57	4420.961 57	215 ± 7	2.6 ± 0.1
2007 Nov 17.005 95	4421.005 95	204 ± 7	2.4 ± 0.1
2007 Nov 17.038 29	4421.038 29	210 ± 7	2.5 ± 0.1
2007 Nov 23.104 48	4427.104 48	255 ± 7	3.1 ± 0.1
2007 Nov 23.130 82	4427.130 82	266 ± 7	3.2 ± 0.1
2007 Nov 23.163 76	4427.163 76	260 ± 7	3.1 ± 0.1
2007 Nov 23.191 62	4427.191 62	274 ± 7	3.3 ± 0.1
2007 Dec 01.956 11	4435.956 11	333 ± 7	4.1 ± 0.1
2007 Dec 02.122 17	4436.122 17	329 ± 7	4.1 ± 0.1
2007 Dec 02.830 04	4436.830 04	338 ± 7	4.2 ± 0.1
2007 Dec 03.023 99	4437.023 99	327 ± 7	4.1 ± 0.1

[a]Separation distance between true nucleus and false nucleus.

(e.g. the false nucleus). With this question in mind, we construct a simple dust model aimed at constraining the possible source (or sources) of emission. We make several simplifying assumptions, as in any model, and do not seek a complete analytical description of the outburst event. Instead, we simply aim to determine whether 17P's nucleus is a plausible origin of the dust in the outer coma, given its significant offset from the coma centre (and the approximate location of the false nucleus) in observations two weeks after the initial outburst and later.

We define the plane of the sky as the x–y plane, where the comet nucleus is located at the origin and the x-axis is perpendicular to the projection of the sunward vector (the positive y-axis) in the plane of the sky. The z-axis is taken to be aligned with the line of sight, with the positive axis extending towards the observer.

Assuming a simplistic model of isotropic emission in which particles are ejected at terminal ejection velocities of v_{ej} in all directions, we expect the coma to be initially spherical and then become paraboloidal as solar radiation pressure applies a uniformly directed acceleration, a_{rp}, to each coma particle (cf. Eddington 1910), Following convention, we parametrize particle size by the dimensionless parameter, β, which is defined as the ratio of a particle's acceleration due to radiation pressure to its acceleration due to solar gravity. Formally, β is a complicated function of the size, composition, and shape of a given dust grain (Burns, Lamy & Soter 1979), though in practice, it can be approximated by $\beta \approx 1/a_d$, where a_d is the radius of a given dust particle in μm.

Using the β parametrization, the acceleration of a particle due to solar radiation pressure is then approximately given by

$$a_{rp} = \beta \frac{g_\odot}{R_{au}^2}, \tag{7}$$

where $g_\odot = 0.006\,\mathrm{m\,s^{-2}}$ is the gravitational acceleration to the Sun at 1 au and R_{au} is the heliocentric distance in au.
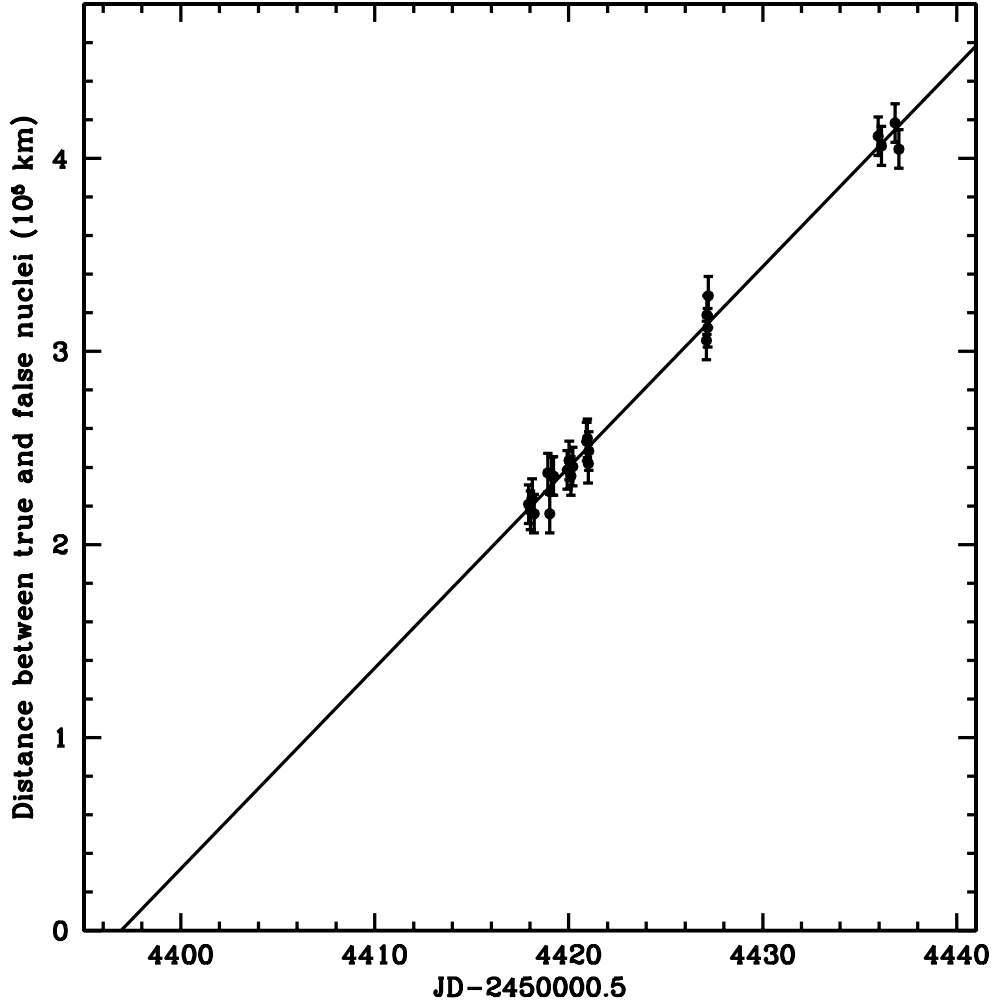
Figure 6. Distance (solid circles) between the nucleus and separated fragment of 17P between 2007 November 5–6 and 2007 December 2–3 (where JD 245 0000.5 = 4400.0 corresponds to 2007 October 27.0), plotted as a function of time. The best linear fit is shown as a solid line.

We adopt a typical particle size-velocity relationship of

$$v_{ej} \sim v_0 \beta^{1/2}, \qquad (8)$$

where v_0 is the reference ejection velocity in m s^{-1} of a particle with $\beta = 1$ (cf. Ishiguro et al. 2007; Hsieh, Jewitt & Ishiguro 2009).

Noting the short distance that the comet travelled around its orbit (from $\nu = 61°3$ to $65°0$; Table 1) during the first 15 d of the outburst (from 2007 October 23.6 to 2007 November 5–6; the period to which we confine our modelling analysis), we make the simplifying approximation of treating the orientation of the solar radiation pressure acceleration vector as constant during this period. The (x, y, z) coordinates of a dust particle, as viewed at opposition, ejected from the nucleus at an elevation angle of θ and azimuth angle of ϕ, are then given by

$$x = v_{ej} t \cos(\theta) \cos(\phi) \qquad (9)$$

$$y = v_{ej} t \cos(\theta) \sin(\phi) \qquad (10)$$

$$z = -\frac{1}{2} a_{rp} t^2 + v_{ej} t \sin(\theta), \qquad (11)$$

which we calculate for $-90° \leq \theta \leq 90°$ and $0° \leq \phi < 360°$ in $1°$ intervals for both θ and ϕ. Then, rotating our coordinate system to

account for a non-zero phase angle, α, at the time of observation, we obtain

$$x' = x \qquad (12)$$

$$y' = y \cos(\alpha) + z \sin(\alpha) \qquad (13)$$

for the (x', y') coordinates (in physical distance) of our test dust particles in the plane of the sky. These coordinates are then divided by the apparent pixel scale to obtain our final (x', y') coordinates in pixels.

In this modelling study, our focus is on the fastest moving particles in the outer envelope of the dust coma, and we are therefore only concerned with the minimum observed particle size in the coma, or β_{max}. Thus, using the geometric circumstances of 17P on 2007 November 5–6, we generate a series of model dust clouds using various values for β and v_0 that satisfy $v_{ej} = 550$ m s^{-1} (i.e. the velocity we derive for particles on the outermost edge of the dust coma).

We find that each of our parameter sets selected in this way produces a nearly circular dust cloud (as projected in the plane of the sky) with a diameter of about 18 arcmin, consistent with the actual size of the dust envelope on 2007 November 5–6 (as expected, given the constraints we applied to our initial parameters). As larger
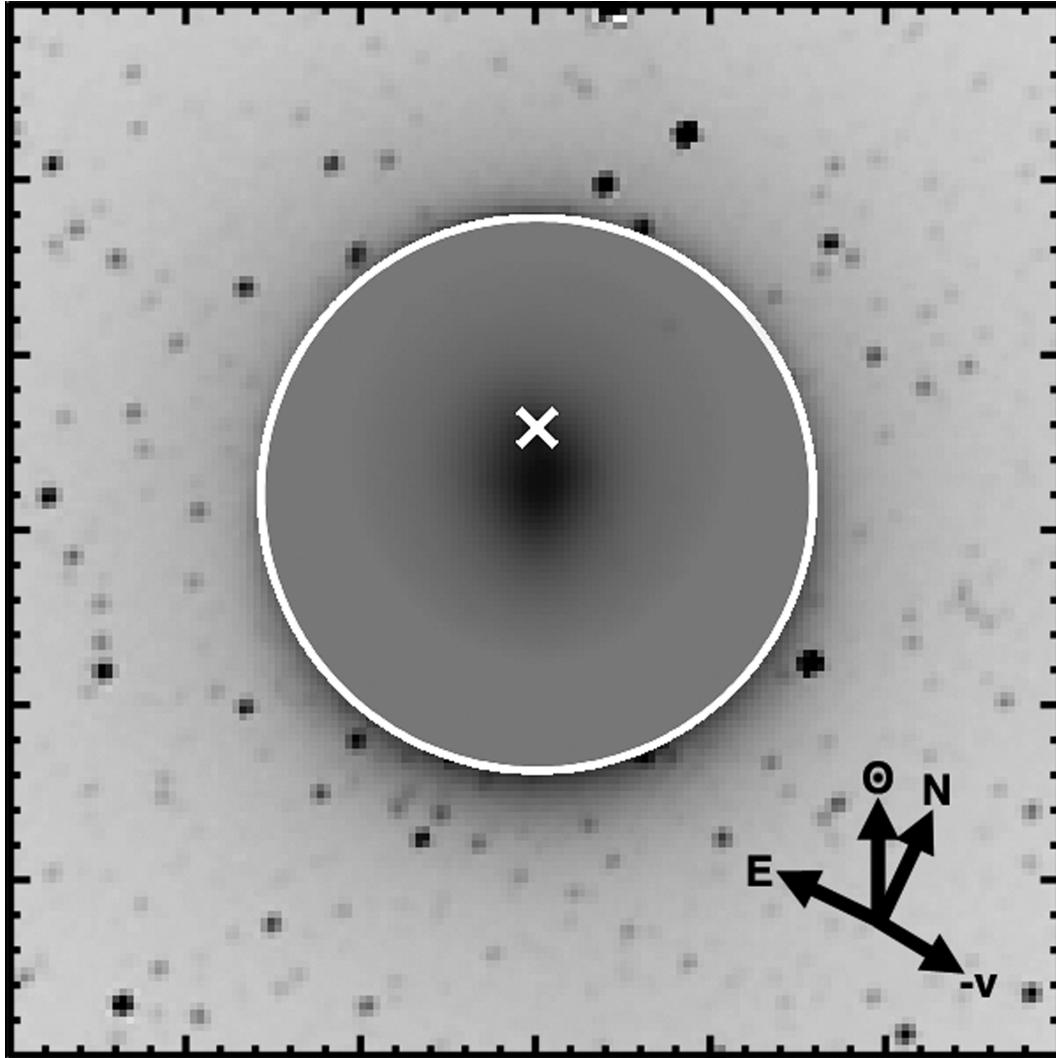
Figure 7. A SuperWASP image of 17P from 2007 November 5–6 with the outer envelope of a modelled dust cloud, marked with a solid white line, overlaid. Different contrast scaling is used for the comet and the sky to emphasize detail in the inner coma. The model dust cloud consists of particles sharing a single β value ejected in a single impulsive event. The origin point of modelled dust emission is marked with an 'X' and coincides with the image of 17P's nucleus in the observed data. The modelled dust envelope was generated using $\beta = 1.0$, $v_0 = 550$ m s^{-1}, $R = 2.49$ au, $\Delta = 1.62$ au, $\alpha = 13°8$, and a pixel scale conversion of 1.61×10^4 km pix^{-1} (corresponding to the SuperWASP pixel scale of 13.7 arcsec pix^{-1}), and is coincident with the outer envelope of the observed dust coma. The image shown is approximately 35×35 arcmin^2 and is oriented such that the sunward vector (as projected in the sky) corresponds to the positive vertical axis.

β and smaller v_0 values are used, the dust cloud remains fixed in size but becomes increasingly offset from the point of emission. Physically, the fixed size of the cloud results from our constraint on v_{ej} described above, while the shifting position of the cloud as β increases corresponds to smaller particles experiencing larger accelerations due to solar radiation pressure. The cloud therefore 'drifts' more quickly relative to the nucleus. In the limiting case of particles with very small β values (i.e. very large particles), solar radiation pressure would not cause the dust to drift at all, and the nucleus would therefore appear to be at the exact centre of the dust cloud.

Assuming 17P's nucleus to be the primary origin point of the particles in the outer dust coma, we find that the model dust cloud that best approximates the relative positions of the nucleus and the observed outer edge of the coma is produced by particles with $\beta = 1.0$ (or $a_d \sim 1$ μm) and $v_0 = 550$ m s^{-1} (Fig. 7). We note that these model parameters are selected to match our observed

expansion rate, and as such, model coma sizes and measured coma sizes agree by definition. The model dust envelopes plotted in Fig. 7 are produced by isotropic emission as described above, but we also note that identical dust envelopes can also be produced by semi-isotropic (i.e. hemispherical) emission solely from either the Sun-facing hemisphere or the non-Sun-facing hemisphere. This finding is consistent with Moreno et al. (2008) who found that the outer shell of the dust coma could be fit by emission from the entire Sun-facing hemisphere of 17P.

As stated above, the simplicity of our model does not allow us to comprehensively explain all aspects of 17P's dust morphology. None the less, we show that, for reasonable dust particle sizes ($a_d \gtrsim 1$ μm), the position of 17P's dust coma relative to the nucleus in the two weeks after the start of the outburst can be accounted for by a single isotropic (or semi-isotropic) emission event where 17P's nucleus is the source of emission. In contrast, particles in a dust cloud for which, for example, a large separated fragment

with the same motion as the false nucleus (cf. Section 3.4) is the emission origin (i.e. where the cloud shows minimal drift relative to its source) would have to have $\beta_{max} = 0.5\,(a_d \gtrsim 2\,\mu\text{m}$; where $v_0 = 780\,\text{m s}^{-1}$).

In terms of particle size constraints, both scenarios are essentially equally plausible, though we note that a more powerful ejection mechanism (to account for the larger value of v_0) is required in the second scenario where emission originates from the false nucleus. Admittedly, even the relatively more modest $v_0 = 550\,\text{m s}^{-1}$ value required for the true nucleus to be the emission source is high, though it is at least not unprecedented; the 1836 outburst of 1P/Halley was characterized by a coma expansion rate of $575\,\text{m s}^{-1}$ (Sekanina 2008b). In terms of outburst mechanics, however, the former scenario is must be considered more likely as it only requires a single explosive outburst taking place on 17P's nucleus, whereas the latter scenario requires a two-part event where a large fragment first detaches at high speed (projected velocity of $\sim 120\,\text{m s}^{-1}$; Section 3.4) from the primary nucleus and then subsequently explosively disintegrates.

3.6 Gas modelling

Sekanina (2008a) and others have cautioned that 17P's dust coma could be significantly contaminated by the gas coma. Kobayashi et al. (2007) observed gas emission bands on 2007 October 25.46, but not on 2007 October 24.58, suggesting that ice grains ejected in the initial outburst did not sublimate until some point in the interim period between their observations. Wagner et al. were able to trace CN (0–0) emission as far as 2.4 arcmin from the photocentre of the dust cloud in observations taken on 2007 October 25.181 and 25.465 (Kobayashi et al. 2007), implying an average velocity of 1.6–1.9 km s^{-1}, consistent with our estimated gas coma expansion velocity of $\gtrsim 1.7$ km s^{-1} (Section 3.2). Schleicher (2009) observed steadily decreasing production rates of several gas species between 2007 November 1 and 2008 March 5.

In terms of our data, it is possible that the portion of 17P's coma surface brightness profile designated Region 3 in our analysis simply fades below the background detection limit. However, we hypothesize that this region in fact corresponds to the comet's gas coma, and that by 2007 November 13–14, this region had disappeared from the coma surface brightness profile because most of the gas molecules initially released had photodissociated or ionized and the remaining coma was below our detection limit.

To test this hypothesis, we construct a simple model of 17P's gas coma based on the Monte Carlo model of Combi & Delsemme (1980) but with additional modifications. First, we assume that the parents have an isotropic Maxwellian velocity distribution with a mean velocity of 0.54 km s^{-1}. This would be expected for a normal comet undergoing steady-state sublimation (Cochran & Barker 1986), though it is possible that this velocity is an underestimate since an explosive release of material could result in higher acceleration of gas from the nucleus than usual. In addition, we have adapted the model to assume either a single outburst in terms of a delta function for the production of gas, or an outburst where the production of parent molecules instantaneously starts at a maximum value and thereafter falls off exponentially. Neither scheme may be accurate in detail, but they allow us to conduct a basic analysis of gross gas coma morphology.

Gas emission in the SuperWASP images was likely dominated by the commonly observed (0–0) band of C_2. The production of this species has been investigated by many investigators due to its

domination of the optical emission spectrum of comets. A recent in-depth study of C_2 chemistry in comet Hale-Bopp by Helbert et al. (2005) concluded that C_2H_2 was the primary parent molecule, but that C_2H_6 was an additional minor parent and electron impact dissociation is important to consider as well as photodissociation. A model including multiple production and destruction mechanisms that properly accounts for relative reaction rates is beyond the scope of this paper. Instead, we adopt a simple two-step single parent photodissociation model as used in the past for other comets. Although Helbert et al. (2005) show such a model is not physically accurate, previous authors have been able to fit C_2 coma profiles with such a scheme by using suitable parameters. Here we assume the photodissociation values found by Lederer, Campins & Osip (2009) of a parent lifetime of $3.4 \times 10^4 R^2$ s, a C_2 daughter lifetime of $1.2 \times 10^5 R^2$ s and an excess C_2 velocity from dissociation of 1.2 km s^{-1}.

In the model we generated 10^9 molecules and calculated the resulting surface brightness profiles for a pulse outburst, one with a 2 d exponential decay time, and one with a 12 d lifetime as suggested from latetime gas measurements by Schleicher (2009) (we note that Schleicher found a faster rate of decay in activity than an exponential). In Fig. 8, we overplot these model profiles on 17P's observed surface brightness profile for the night of 2007 October 31–November 1, scaling the model plots vertically (i.e. varying the column density of the modelled gas emission) in order to produce the best possible fit to the observed surface brightness profile in the gas-dominated region. As can be seen, we find that the single pulse model offers an excellent fit to the Region 3 portion of the coma surface brightness profile. By contrast, the suitability of the 2 d pulse model is considerably worse as it produces a profile that is too steep, regardless of scaling, to match the observed profile. The 12-d pulse model produces an even steeper profile and therefore an even worse fit.

Taking the single-pulse model as best fitting the outer coma as observed in our images, we note that the expected lifetime of the C_2 coma generated in the initial outburst event is $\sim 10^6$ s or ~ 13 d. This expected lifetime is consistent with an outer gas coma that is visible as Region 3 in our images up to 2007 November 5–6 (14 d after outburst), but is absent in images obtained from 2007 November 13 to 14 onwards (22 d after outburst).

4 DISCUSSION AND SUMMARY

4.1 Primary findings

Wide-field imaging of the 2007 outburst of 17P/Holmes was serendipitously obtained by the SuperWASP-North facility on 17 nights over a 42-night period beginning on the night (2007 October 22–23) immediately prior to the outburst. We report the following key findings:

(i) The comet was not detected in data from the night before the outburst's discovery on the night of 2007 October 22–23, indicating that it remained below the SuperWASP detection threshold of $m_V \sim 15$ mag (consistent with pre-outburst reports placing the comet's brightness at $m_V \sim 17$ mag) until at least 2007 October 23.3.

(ii) The unresolved coma (as seen by SuperWASP) was likely optically thin during our observations on the first night of the outburst. The comet's light curve during these observations is consistent with an exponential function, suggesting that its rapid brightening could have been driven by the progressive fragmentation of ejected material produced on a very short time-scale at the time of the
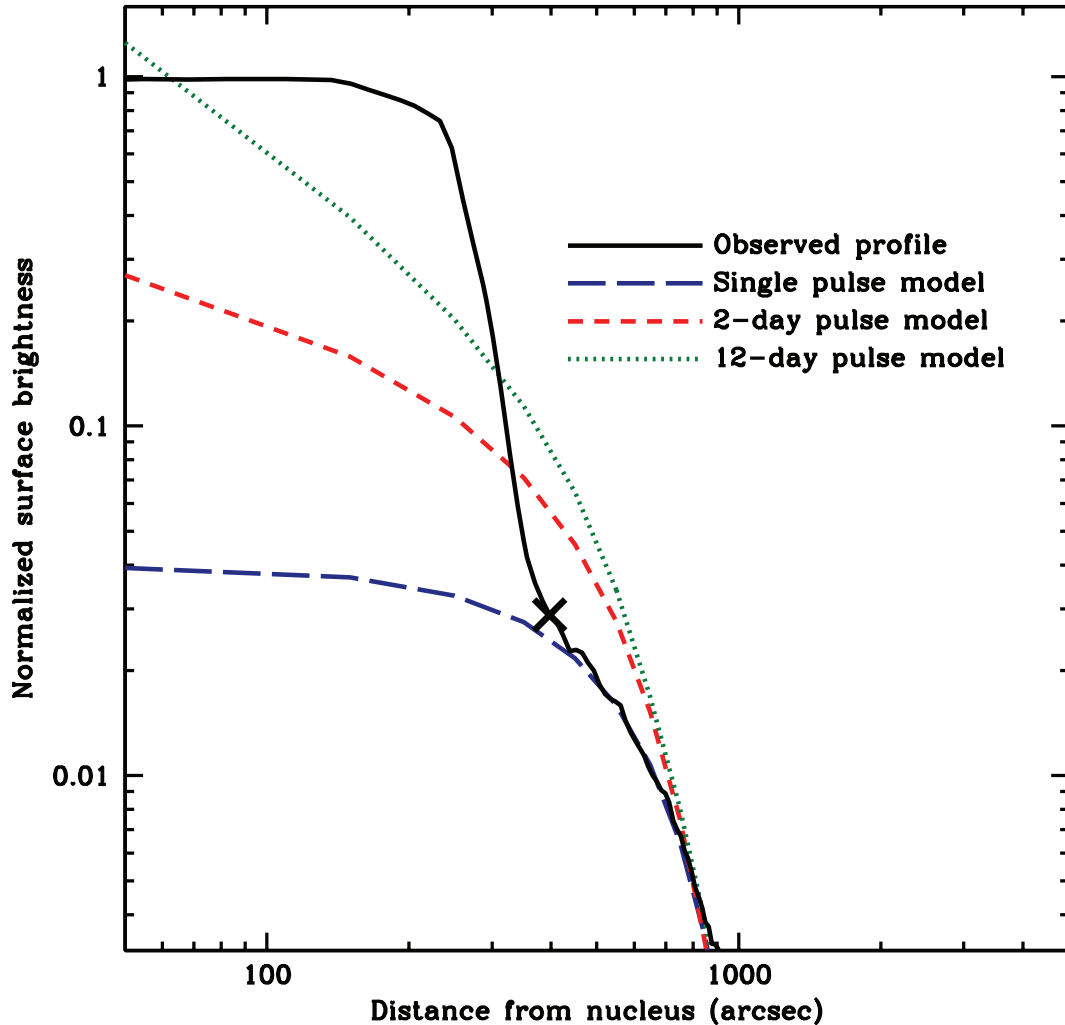
Figure 8. Comparison of the observed surface brightness profile of the coma of 17P (solid line) on the night of 2007 October 31–November 1 (cf. Fig. 4a), and plots of modelled C_2 column density. The point where the observed coma transitions from dust-dominated to gas-dominated is marked by 'X'. Large-dashed line: precursor molecules are all released from the nucleus in a single pulse on 2007 October 23.6. Small-dashed line: the release of precursor molecules begins on 2007 October 23.6 but then exponentially decreases with a 48-h time-scale. Dotted line: as above with the gas production exponentially decreasing with a 12 d time-scale. Model profiles have been scaled vertically to produce the best possible fit to the observed coma profile.

initial outburst. Our best-fitting functions to the data imply an initial fragmentation time-scale of $t_{frag} \sim 2 \times 10^3$ s, decreasing to $t_{frag} \sim 1 \times 10^3$ s, and a near-instantaneous leap in brightness from a magnitude of $m_V \sim 17$ to $\sim$11 mag at the moment of the initial outburst.

(iii) Analysis of coma surface brightness profiles reveals a velocity gradient consistent with the outer coma being dominated by material ejected in an explosive manner (i.e. at a single instant), rather than over an extended period of time. Near the outer edge of the visible coma, where the coma likely transitions from being dust-dominated to gas-dominated, this velocity gradient corresponds to an expansion velocity of 0.55 ± 0.02 km s^{-1}, consistent with previous reported measurements. From this analysis, we find a most likely outburst date of $t_0 = 2007$ October 23.3 ± 0.3. This finding of explosively ejected material dominating the outer coma does not rule out the possibility of subsequent sustained mass ejection supplying the inner coma at later times.

(iv) We measure the rate of motion (relative to the nucleus) of the secondary brightness peak in 17P's coma, which we refer to as the

'false nucleus', and find a projected drift velocity of $v_{drift} = 120 \pm 5$ m s^{-1}, consistent with previously reported measurements.

(v) Dust modelling shows that 17P's nucleus is a plausible primary emission source of outer coma material, and that a secondary source such as a separated nucleus fragment is not required to explain the motion of the coma relative to the nucleus. We show instead that the drifting of the coma relative to the nucleus can be explained as the consequence of radiation pressure alone.

(vi) Modelling of 17P's gas coma indicates that the morphology of the portion of the observed coma profile hypothesized to be gas extending past the outer dust coma is best explained by a single, instantaneous outburst of gas production, rather than extended gas production that persists over several days. This result is consistent with our conclusion that the outer dust coma is likely dominated by material ejected instantaneously, and not over an extended period of time. We also note that C_2 is likely to be the dominant observed component of the gas coma, and find that its decay time is consistent with SuperWASP observations of the disappearance of the observed coma profile region attributed to gas.

4.2 Anatomy of an outburst

To date, no consensus has emerged to explain the physical origin of 17P's spectacular outbursts in 1892 and 2007. A primary difficulty lies in reconciling the occurrence of such an apparently catastrophic event at least twice in the recent past with a lack of comparable outbursts in almost all other comets, although Sekanina (2008b) has noted that 1P/Halley exhibited a similarly powerful outburst in 1836. Whipple (1984) suggested that a grazing encounter and eventual impact by a small satellite with the nucleus could have been responsible for the 1892 outburst, but such an explanation was rendered highly implausible with a second episode of outburst activity in 2007. Furthermore, any model formulated to explain 17P's behaviour must also account for the lack of outburst activity in the 115 yr between 1892 and 2007 (Sekanina 2009b).

Sekanina (2008a,b) has proposed a scenario in which an inwardly diffusing thermal wave gradually penetrated a large, weakly cemented pancake-shaped layer of the nucleus (analogous to those observed for 9P/Tempel 1; cf. Thomas et al. 2007) over numerous orbits until it finally reached a large reservoir of amorphous water ice at the layer's base. Upon being heated to the necessary transition temperature, this amorphous ice layer underwent an exothermic transformation to crystalline ice, leading to rapid sublimation and causing the pancake-shaped layer to separate from the nucleus, receding at a relative velocity of ~ 1 m s^{-1}, and almost immediately explosively disintegrate.

We note that our dust modelling (Section 3.5) shows that it is not necessary for a separated fragment to be the source of emission to explain the position of the outer dust coma relative to the true nucleus. Thus a model where a large surface fragment first separates from the nucleus and then explosively disintegrates, requiring two non-simultaneous catastrophic events, may be needlessly complicated. There could still be concentrations of material related to large fragments ejected in the initial outburst that then disintegrated (e.g. Stevenson et al. 2010), but these may be better characterized as byproducts, rather than key components, of the outburst.

Altenhoff et al. (2009) propose an alternate hypothesis in which a particularly close perihelion passage by 17P on 2007 May 4 substantially raised the sublimation rate of subsurface water ice relative to previous perihelion passages. This increased production of subsurface water vapour, coupled with an 'airtight' layer of surface regolith, ultimately led to an explosive disintegration of 17P's dust mantle 172 d later, causing the observed outburst. While it is true that 17P's perihelion passage just 2.05 au from the Sun was its closest approach to the Sun in over a century (according to JPL's Horizons ephemeris generator at http://ssd.jpl.nasa.gov/horizons.cgi), we note that 17P's perihelion distance immediately prior to its 1892 outburst was a more modest 2.14 au from the Sun, a distance comparable to perihelion passage distances in 1864, 1871, 1878, 1885, 1899, 1906, 1972, 1979, 1986, 1993 and 2000, all of which were reached without any recorded reports of behaviour comparable to the comet's 1892 or 2007 outbursts.

Most recently, Reach et al. (2010) propose a scenario in which trapped gases released by the crystallization of amorphous ice, as well as sublimation of other ices driven by the exothermic crystallization process, cause a build up of gas pressure in a subsurface cavity on the comet. The outburst of 17P then occurred when the pressure built up within this cavity exceeded the strength of the surrounding material (found to be relatively high – 10–100 kPa – based on the nucleus's survival of the outburst), causing the cavity to rupture violently and energetically, creating the observed explosive ejection of nuclear material. We note that while Kossacki & Szutowicz (2010) report that the crystallization of amorphous water ice is unlikely to have caused 17P's outburst, they reach this conclusion based on a simple model in which the ice being crystallized is present in a subsurface layer just below a dust mantle. The hypothesis presented by Reach et al. is based on a different physical scenario where ice crystallization occurs in a subsurface void in which gas pressure is able to build up, and as such, we believe that it remains plausible and, of the hypotheses proposed thus far, is the most consistent with our own findings. We note, however, that it then raises questions as to why 17P is the only comet known thus far with the apparently unique combination of high-tensile-strength nuclear material, subsurface cavities and amorphous ice capable of driving two of the largest cometary outbursts observed in modern astronomy.

Gaillard et al. (2007) reported that observations they made between 2007 October 24 and 2007 November 4 with the Pic du Midi 1 m telescope show multiple dust streams with well-defined origin points, four of which were measured to recede from 17P's nucleus at roughly constant velocities (as projected on the sky) ranging from 50 to 100 m s^{-1}, implying the presence of unresolved, steadily disintegrating nucleus fragments in the coma. These fragments were also calculated to have separated from the nucleus between 2007 October 23.7 and 2007 October 24.8. Additionally, Stevenson et al. (2010) observed at least sixteen 10- to 100-m-scale fragments receding from the nucleus that showed evidence of ongoing sublimation and disintegration. Coupled with our finding of dust fragmentation in the first hours after outburst, these observations point to a scenario of continued fragmentation of cometary material following the outburst.

We certainly still have far from a complete picture of 17P's 2007 outburst. We suggest that detailed dust modelling and analysis of images of the comet's inner coma using data with higher spatial resolution than SuperWASP would be useful for clarifying the temporal and kinematic nature of the outburst, in particular whether significant dust production continued from the nucleus after the initial outburst event and, if so, whether ejection velocities were comparable to those in the initial outburst event. More detailed discussions of spectroscopy would also help constrain the spatial and temporal nature of the contribution of gaseous species to the 17P's appearance, such as whether sublimation of nucleus-bound ices or ice particles in the coma was significant, and whether there was any appreciable delay in the sublimation of icy material in the coma that could be linked to hierarchical fragmentation of macroscopic nucleus particles.

REFERENCES

Altenhoff W. J., Kreysa E., Menten K. M., Sievers A., Thum C., Weiss A., 2009, A&A, 495, 975

Bockelée-Morvan D. et al., 2008, ApJ, 679, L49

Burns J. A., Lamy P. L., Soter S., 1979, Icarus, 40, 1

Buzzi L., Muler G., Kidger M., Henríquez Santana J. A., Naves R., Campas M., Kugel F., Rinner C., 2007, IAU Circular, 8886, 1

Casali M. et al., 2007, Minor Planet Electronic Circulars, 2007-U69

Cochran A. L., Barker E., 1986, ESA SP-250 Vol. 1. ESA, Noordwijk, p. 439

Combi M. R., Delsemme A. H., 1980, ApJ, 237, 633

Dello Russo N., Vervack R. J. Jr, Weaver H. A., Montgomery M. M., Deshpande R., Fernández Y. R., Martin E. L., 2008, ApJ, 680, 793

Drahus M., Paganini L., Ziurys L., Peters W., Soukup M., Begam M., 2007, IAU Circular, 8891, 1

Eddington A. S., 1910, MNRAS, 70, 442

El-Houssieny E. E., Nemiroff R. J., Pickering T. E., 2010, Ap&SS, in press, preprint (arXiv:0908.1450v1)

Fitzsimmons A., Snodgrass C., Southworth J., 2007, IAU Circular, 8887, 3

Gaillard B., Lecacheux J., Colas F., 2007, Cent. Bureau Electron. Telegrams, 1123, 1

Helbert J., Rauer H., Boice D. C., Huebner W. F., 2005, A&A, 442, 1107

Ho T.-M., Thomas N., Boice D. B., Combi M., Soderblom L. A., Tenishev V., 2007, Planet. Space Sci., 55, 974

Hsieh H. H., Fitzsimmons A., Pollacco D. L., 2007, IAU Circular, 8897, 1

Hsieh H. H., Jewitt D., Ishiguro M., 2009, AJ, 137, 157

Ishiguro M., Sarugaku Y., Ueno M., Miura N., Usui F., Chun M.-Y., Kwon S. M., 2007, Icarus, 189, 169

Ishiguro M. et al., 2010, ApJ, 714, 1324

Joshi U. C., Ganesh S., Baliyan K. S., 2010, MNRAS, 402, 2744

Kobayashi H., Kawakita H., Nishikoji A., 2007, IAU Circular, 8887, 1

Kossacki K. J., Szutowicz S., 2010, Icarus, 207, 320

Lamy P. L., Toth I., Fernandez Y. R., Weaver H. A., 2004, Comets II. Univ. of Arizona Press, Tucson, AZ, p. 223

Lederer S. M., Campins H., Osip D. J., 2009, Icarus, 199, 484

Lin Z.-Y., Lin C.-S., Ip W.-H., Lara L. M., 2009, AJ, 138, 625

Meech K. J., Jewitt D. C., 1987, A&A, 187, 585

Montalto M., Riffeser A., Hopp U., Wilke S., Carraro G., 2008, A&A, 479, L45

Moreno F., Ortiz J. L., Santos-Sanz P., Morales N., Vidal-Núñez M. J., Lara L. M., Gutiérrez P. J., 2008, ApJ, 677, L63

Pittichová J., Sekanina Z., Birkle K., Boehnhardt H., Engels D., Keller P., 1997, Earth Moon Planets, 78, 329

Pollacco D. L. et al., 2006, PASP, 118, 1407

Reach W. T., Vaubaillon J., Lisse C. M., Holloway M., Rho J., 2010, Icarus, 208, 276

Schleicher D., 2007, IAU Circular, 8889, 1

Schleicher D., 2009, ApJ, 138, 1062

Sekanina Z., 2008a, Int. Comet Q., 30, 3

Sekanina Z., 2008b, Int. Comet Q., 30, 63

Sekanina Z., 2009a, Int. Comet Q., 31, 5

Sekanina Z., 2009b, Int. Comet Q., 31, 45

Snodgrass C. et al., 2007, Cent. Bureau Electron. Telegrams, 1111, 1

Snodgrass C., Lowry S. C., Fitzsimmons A., 2008, MNRAS, 385, 737

Sposetti S. et al., 2007, Minor Planet Electronic Circulars, 2007-U93

Stevenson R., Kleyna J., Jewitt D., 2010, AJ, 139, 2230

Thomas P. C. et al., 2007, Icarus, 187, 4

Trigo-Rodriguez J. M. et al., 2007, Cent. Bureau Electron. Telegrams, 1118, 1

Trigo-Rodriguez J. M., Davidsson B., Montanes-Rodriguez P., Sanchez A., Troughton B., 2008, Lunar and Planetary Institute Conference Abstracts Vol. 39, All-Sky Cameras Detection and Telescope Follow-Up of the 17P/Holmes Outburst. p. 1627

Tuzzolino A. J. et al., 2004, Sci, 304, 1776

Wagner R. M., Starrfield S., Schwarz G., Larson S., Kaitchuck R., Childers J., Turner G., 2007, IAU Circular, 8887, 2

Whipple F. L., 1984, Icarus, 60, 522

Yang B., Jewitt D., Bus S. J., 2009, AJ, 137, 4538

This paper has been typeset from a TEX/LATEX file prepared by the author.